retention time of authentic LTE_4 were dried and resuspended in assay buffer, which was supplied in the Leukotriene C4/D4/E4 enzyme-immunoassay system (Amersham, Buckinghamshire, UK). Urinary LTE_4 concentrations determined by EIA were corrected for recovery of $[^3H]-LTE_4$. The urinary LTE_4 level was expressed as pg/mg creatinine.

Measurement of $11DTXB_2$

The $11DTXB_2$ was extracted from an acidified sample by adding an equal volume of octadecylsilyl silica powder (ODS) suspension (80 mg/mL in 40% ethanol) followed by mixing, centrifuging (at 2000 g for 3 min at room temperature) and either decanting or aspirating. The pellet was washed with an acidic alcohol solution and then with petroleum ether for deproteinizing and defatting. The $11DTXB_2$ was eluted by ethyl acetate. The pooled ethyl acetate was evaporated to dryness with nitrogen gas. The dried residue, containing $11DTXB_2$, was dissolved in the eluent (acetonitril : chloroform : acetic acid, 10 : 90 : 0.5, v/v/v) and applied to the open silica mini column (Bond Elute SI; VARIAN, Palo Alto, CA, USA). The column was washed with the eluent (acetonitril : chloroform : acetic acid, 20 : 80 : 0.5, v/v/v). The elution buffer, containing the $11DTXB_2$, was dried with nitrogen gas and the amount of $11DTXB_2$ was quantitated by RIA (11-Dehydrothromboxane B2 [^{125}I] RIA kit; Perkin Elmer Life and Analytical Sciences, Boston, MA, USA). The urinary $11DTXB_2$ level was also expressed as pg/mg creatinine.

Statistical analyses

The Mann–Whitney unpaired U-test was used to compare controls and asthmatic children during the stable condition and the Wilcoxon paired test was used to compare asthmatic children during the stable condition and during an acute attack. Correlation was analyzed by Pearson correlation analysis. The percentage of changes was calculated using the following equation: % change = (level during stable condition − level during attack) × 100/level during attack. Data are expressed as the median (range) and $P < 0.05$ was considered significant.

RESULTS

Urinary LTE_4 and $11DTXB_2$ levels

Urinary levels of LTE_4 and $11DTXB_2$ were measured to define the potential roles of CysLTs and TXA_2 in children with bronchial asthma.

Leukotriene E_4 was measured by EIA. Urinary LTE_4 levels are plotted in Fig. 1. Urinary LTE_4 levels in asthmatic children during the stable condition (332 (128–965) pg/mg creatinine) was significantly higher ($P < 0.05$) than that of control subjects (233 (103–389) pg/mg creatinine; Fig. 1a). Comparing the different conditions of asthma, LTE_4 levels during an acute attack (476 (191–1100) pg/mg creatinine) were significantly higher ($P < 0.05$) than those during the stable condition (Fig. 1b).

11-Dehydro-thromboxane $B_2$was measured by RIA and was detectable in all urine samples. Urinary $11DTXB_2$ levels are shown in Fig. 2. Urinary $11DTXB_2$ levels in asthmatic children during the stable condition (1009 (46–6070) pg/mg creatinine) were significantly higher ($P < 0.05$) than those of control subjects (252 (41–716) pg/mg creatinine; Fig. 2a). However, there was no significant difference in $11DTXB_2$ levels during an acute attack (1666 (110–5105) pg/mg creatinine) and during the stable condition (Fig. 2b).

Urinary levels of LTE_4 and $11DTXB_2$ were observed during the stable condition, an acute attack and 2 days after treatment in nine asthmatic children (Fig. 3). Urinary LTE_4 increased from 373 pg/mg creatinine (range 183–556 pg/mg creatinine) during the stable condition to 546 pg/mg creatinine (range 280–1100 pg/mg creatinine) during an acute asthma attack and then decreased to 443 pg/mg creatinine (range 156–872 pg/mg creatinine) 2 days after treatment (Fig. 3a). In contrast, urinary $11DTXB_2$ levels exhibited different patterns after an attack. Urinary $11DTXB_2$ levels increased from 1009 pg/mg creatinine (range 131–2106 pg/mg creatinine) during the stable condition to 1285 pg/mg creatinine (range 166–3122 pg/mg creatinine) during an acute asthma attack and gradually decreased to 842 pg/mg creatinine (range 492–2708 pg/mg creatinine) 2 days after treatment. However, each patient showed variable levels of urinary $11DTXB_2$ 2 days after treatment (Fig. 3b).

Correlations between urinary LTE_4 and $11DTXB_2$

We assessed the relationship between LTE_4 and $11DTXB_2$ in children with bronchial asthma (Fig. 4). No relationship was noted between these prostanoids in children with bronchial asthma or in the controls. In plots of changes from levels observed during an attack to
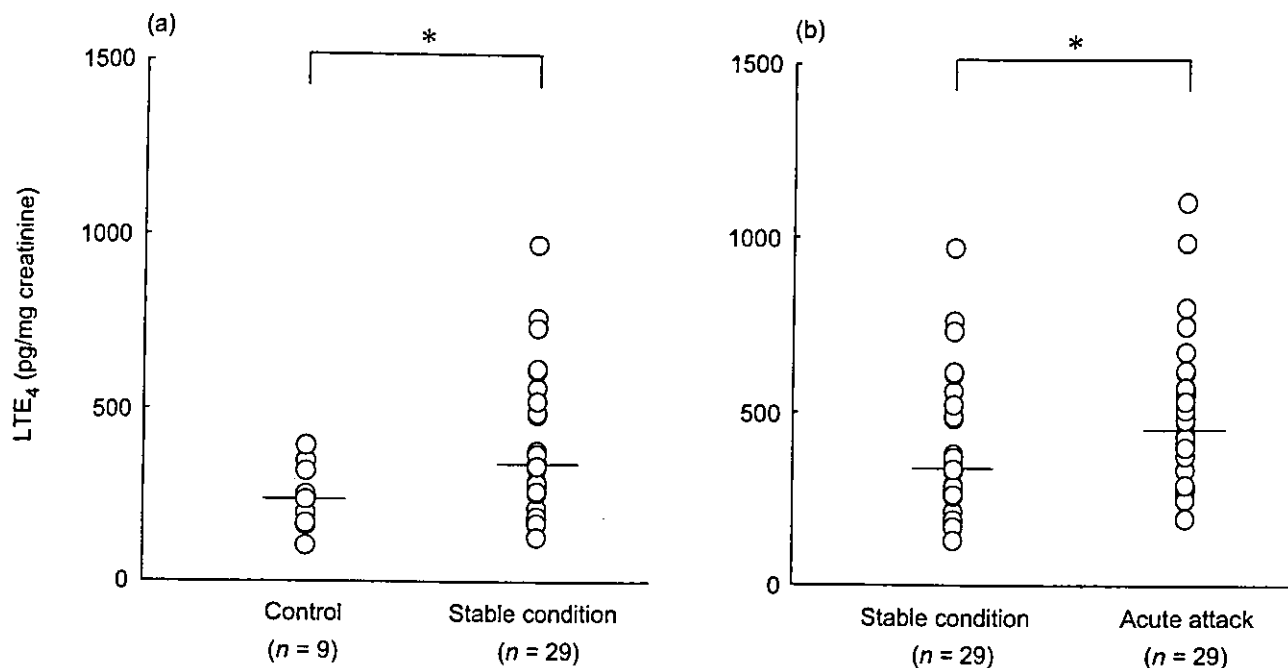
Fig. 1 (a) Urinary leukotriene E_4 (LTE_4) levels in asthmatic children during the stable condition (median 332 pg/mg creatinine; range 128–965 pg/mg creatinine) and in controls (median 233 pg/mg creatinine; range 103–389 pg/mg creatinine). (b) Urinary LTE_4 levels in asthmatic children during an acute asthma attack (median 476 pg/mg creatinine; range 191–1100 pg/mg creatinine) and during the stable condition (median 332 pg/mg creatinine; range 128–965 pg/mg creatinine). Horizontal bars indicate median values. *$P < 0.05$.
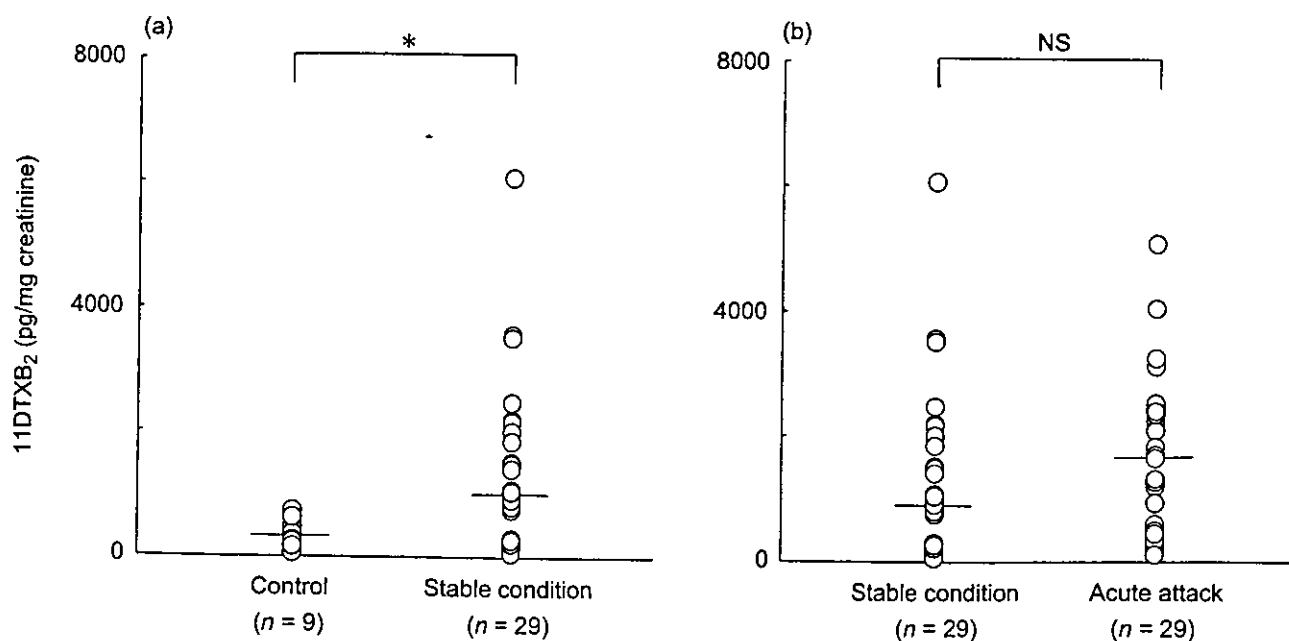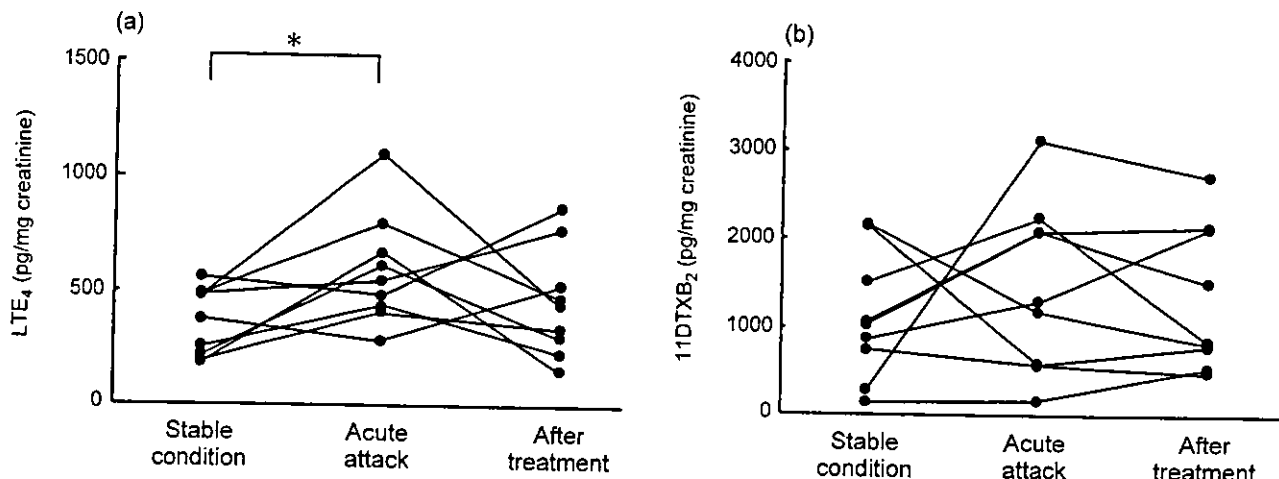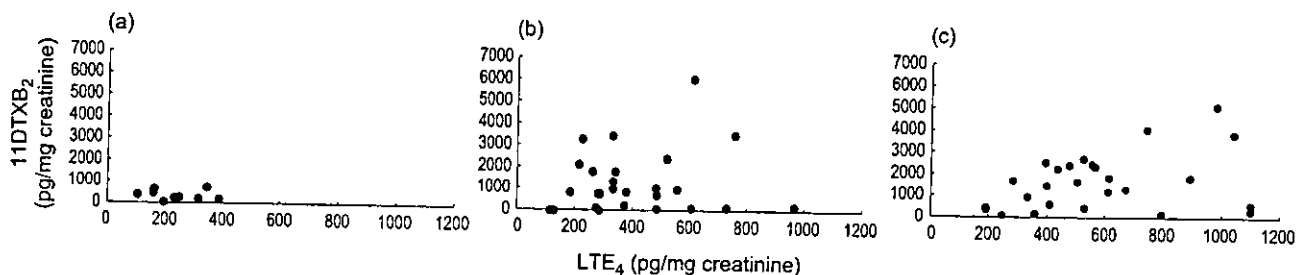

Fig. 2 (a) Urinary 11-dehydro-thromboxane B_2 ($11DTXB_2$) levels in asthmatic children during the stable condition (median 1009 pg/mg creatinine; range 46–6070 pg/mg creatinine) and in controls (median 252 pg/mg creatinine; range 41–716 pg/mg creatinine). (b) Urinary $11DTXB_2$ levels in asthmatic children during an acute asthma attack (median 1666 pg/mg creatinine; range 110–5105 pg/mg creatinine) and during the stable condition (median 1009 pg/mg creatinine; range 46–6070 pg/mg creatinine). Horizontal bars indicate median values. *$P < 0.05$.

Fig. 3 Urinary leukotriene E_4 (LTE$_4$) and 11-dehydro-thromboxane B_2 (11DTXB$_2$) levels in nine children with bronchial asthma during the stable condition, an acute asthma attack and 2 days after treatment. (a) Urinary LTE$_4$ levels increased from a median of 373 pg/mg creatinine (range 183–556 pg/mg creatinine) during the stable condition to 546 pg/mg creatinine (range 280–1100 pg/mg creatinine) during an acute asthma attack, decreasing again to 443 pg/mg creatinine (range 156–872 pg/mg creatinine) 2 days after treatment. (b) Urinary 11DTXB$_2$ levels were apt to increase from a median of 1009 pg/mg creatinine (range 131–2166 pg/mg creatinine) during the stable condition to 1285 pg/mg creatinine (range 166–3122 pg/mg creatinine) during an acute asthma attack and then decrease slowly to 842 pg/mg creatinine (range 492–2708 pg/mg creatinine) 2 days after treatment. *$P < 0.05$.

Fig. 4 Relationship between urinary leukotriene E_4 (LTE$_4$) and 11-dehydro-thromboxane B_2 (11DTXB$_2$) levels. No relationship was noted between these prostanoids in (a) control subjects, (b) asthmatic children while in the stable condition and (c) asthmatic children during an acute asthma attack.

levels during the stable condition, the changes in LTE$_4$ were not related to changes in 11DTXB$_2$ in children with bronchial asthma (Fig. 5). Neither gender, age, serum IgE nor eosinophil count had any relationship with urinary levels of LTE$_4$ or 11DTXB$_2$ (data not shown). One patient (no. 5) had high eosinophil counts (1344/μL during the stable condition; 871/μL during an acute attack; and 2567/μL when he felt better 2 days after treatment). However, the eosinophil count did not correlate with urinary levels of LTE$_4$ or 11DTXB$_2$. There was no significant correlation between urinary levels of LTE$_4$ and the severity of asthma; however, the severity of asthma in

patients with high levels of urinary LTE$_4$ were classified as 'moderate persistent' or 'severe persistent'.

Discussion

Cysteinyl leukotrienes and TXA$_2$ are considered to play important roles in the pathogenesis of bronchial asthma. The relationship between urinary LTE$_4$ and 11DTXB$_2$ in the pathogenesis of asthma has been reported by several investigators;[2-5,8,11,13,20] because of the instability of CysLTs and TXA$_2$, the end-products of the cascade were determined. However, most studies have been
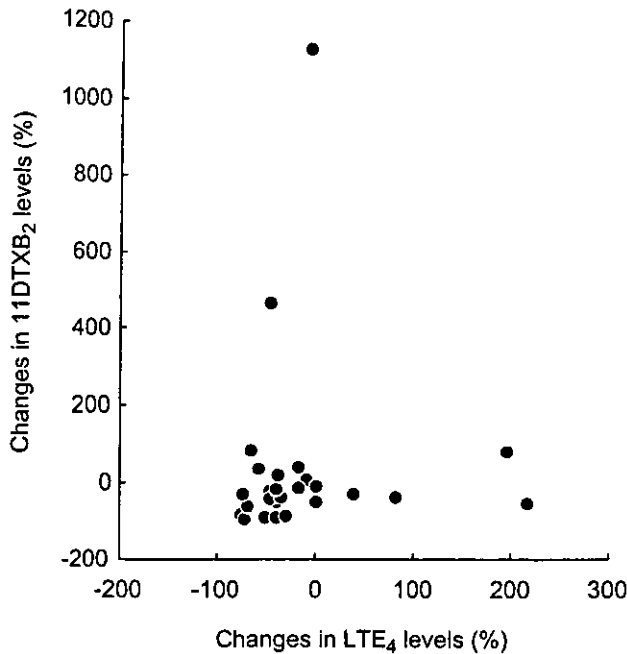
Fig. 5 Changes (%) in leukotriene E_4 (LTE_4) levels did not correlate with changes (%) in 11-dehydro-thromboxane B_2 ($11DTXB_2$) levels in children with bronchial asthma. The percentage change was calculated as follows: (level during stable condition – level during attack) × 100/level during attack.

performed in adults. In the present study, we have demonstrated the relationship between urinary LTE_4 and $11DTXB_2$ in children with bronchial asthma.

In the present study, urinary LTE_4 levels in children with bronchial asthma during the stable condition were significantly higher than in control children. In addition, urinary LTE_4 levels in children during an acute asthma attack were higher than during the stable condition. Asano et al.[5] also demonstrated that patients with mild to moderate asthma excrete LTE_4 in the urine at a greater rate than control subjects. Taylor et al.[4] revealed that urinary LTE_4 was significantly higher in asthma patients after antigen challenge than in control subjects. The results of the present study are consistent with previous findings in adult asthmatic patients.[3,4,9,11,17,20]

In the present study, urinary $11DTXB_2$ levels were higher in children with bronchial asthma than in controls. Unlike LTE_4, urinary $11DTXB_2$ levels did not increase markedly during an acute attack.

Oosaki et al.[3,20] reported on variations in urinary levels of these mediators in patients with spontaneous asthma attacks who were monitored for 3 days and whose state improved. The study of Oosaki et al.[3,20]

showed that urinary levels of LTE_4 were significantly higher during the attack and returned to control levels once the patient's state had improved. In the present study, the urinary levels of these prostanoids were measured in asthmatic children during the stable condition, during an acute attacks and 2 days after treatment. In eight children, urinary LTE_4 levels increased during an acute attack and decreased 2 days after treatment. One patient (no. 8) exhibited a different pattern of urinary LTE_4 excretion: levels decreased during an acute attack and then increased when she felt better 2 days after treatment. However, the urinary $11DTXB_2$ levels in this patient increased during an acute attack and then decreased 2 days after treatment. This patient had atopic-type bronchial asthma and was treated with theophyline, steroid inhalant, DSCG and a β_2-adrenergic receptor agonist. Before she was enrolled in the study, she had been treated with an LTRA for 5 weeks. However, LTRA treatment had little effect on her asthma. Urinary $11DTXB_2$ levels tended to increase during an asthma attack and persisted 2 days after treatment. Similar to the findings of the present study, Oosaki et al. have shown that the median level of urinary $11DTXB_2$ was highest during the 3rd hospital day in atopic-type patients and during the 2nd hospital day in non-atopic-type patients.[3]

In the present study, urinary levels of LTE_4 and $11DTXB_2$ were slightly higher than those reported previously.[2-5,8,11,13,20] Osamura et al. had reported that urinary levels of $11DTXB_2$ were significantly high between 1 and 3 years after birth and that they tended to decrease gradually with age thereafter.[21] Because all our subjects were children (1–15 years of age), this may explain why the urinary levels of $11DTXB_2$ were slightly higher in the present study than those reported previously.

Suzuki et al.[2] reported that no significant relationship was observed between urinary LTE_4 and $11DTXB_2$ in asthmatic patients. Oosaki et al.[3] also examined the relationship in changes (%) between these two metabolites; however, they noted no significant difference. In the present study, consistent with results of previous studies, no relationship was observed between urinary LTE_4 and $11DTXB_2$ in children with bronchial asthma. In addition, changes (%) in LTE_4 levels were not associated with $11DTXB_2$ levels in children with bronchial asthma. This suggests that increases in the levels of these two metabolites are not correlated with one another.

Neither gender, age, serum IgE nor eosinophil count revealed any relationship with urinary levels of LTE_4 or $11DTXB_2$. Eosinophils play an important role in the

pathogenesis of bronchial asthma and the eosinophil count is correlated with the clinical severity of the disease.[22] However, there are few studies referring to the correlation between eosinophil count and urinary levels of LTE_4 or $11DTXB_2$. There was no significant correlation between urinary levels of LTE_4 and the severity of asthma; however, the severity of the asthma in patients with high levels of urinary LTE_4 tended to be classified as 'moderate persistent' or 'severe persistent'.

In conclusion, we have shown significantly higher levels of urinary LTE_4 and $11DTXB_2$ in asthmatic children during the stable condition. These findings strongly suggest that the arachidonate cascade metabolites CysLTs and thromboxanes play certain roles in the pathogenesis of bronchial asthma in children. According to the differential changes in urinary levels of these metabolites during an acute attack, we suppose that an imbalance in the metabolism arises between the 5-lipoxgenase pathway and the cyclooxygenase pathway. The measurement of LTE_4 and $11DTXB_2$ in urine samples, which is a safe and easily available method of estimating the synthesis and release of the mediator in children, would be useful in understanding the pathogenesis of bronchial asthma.

REFERENCES

1   Samuelsson B. Leukotrienes: Mediators of immediate hypersensitivity reactions and inflammation. *Science* 1983; **220**: 568–75.
2   Suzuki N, Hishinuma T, Abe F et al. Difference in urinary LTE_4 and 11-dehydro-TXB_2 excretion in asthmatic patients. *Prostaglandins Other Lipid Mediat.* 2000; **62**: 395–403.
3   Oosaki R, Mizushima Y, Kawasaki A, Mita H, Akiyama K, Kobayashi M. Correlation among urinary eosinophil protein X, leukotriene E_4, and 11-dehydrothromboxane B_2 in patients with spontaneous asthmatic attack. *Clin. Exp. Allergy* 1998; **28**: 1138–44.
4   Taylor GW, Taylor I, Black P et al. Urinary leukotriene E_4 after antigen challenge and in acute asthma and allergic rhinitis. *Lancet* 1989; i: 584–8.
5   Asano K, Lilly CM, OíDonnell WJ et al. Diurnal variation of urinary leukotriene E_4 and histamine excretion rates in normal subjects and patients with mild-to-moderate asthma. *J. Allergy Clin. Immunol.* 1995; **96**: 643–51.
6   Inoue R, Fukao T, Kato Y, Teramoto T, Utsumi M, Kondo N. Time-course study of the levels of urinary leukotriene E_4, serum thromboxane B_2 and serum eosinophil cationic protein in spontaneous asthma attacks in five children. *J. Invest. Allergol. Clin. Immunol.* 1999; **9**: 361–6.
7   Taylor IK, Ward PS, O'Shaughnessy KM et al. Thromboxane A_2 biosynthesis in acute asthma and after antigen challenge. *Am. Rev. Respir. Dis.* 1991; **143**: 119–25.

8   Sladek K, Dworski R, Fitzgerald GA et al. Allergen-stimulated release of thromboxane A_2 and leukotriene E_4 in humans. Effect of indomethacin. *Am. Rev. Respir. Dis.* 1990; **141**: 1441–5.
9   Westlund P, Granstrom E, Kumlin M, Nordenstrom A. Identification of 11-dehydro-TXB_2 as a suitable parameter for monitoring thromboxane production in the human. *Prostaglandins* 1986; **31**: 929–60.
10   Roberts 2nd LJ, Sweetman BJ, Oates JA. Metabolism of thromboxane B_2 in man. Identification of twenty urinary metabolites. *J. Biol. Chem.* 1981; **256**: 8384–93.
11   Kumlin M, Dahlén B, Björck T, Zetterström O, Granström E, Dahlén SE. Urinary excretion of leukotriene E_4 and 11-dehydro-thromboxane B_2 in response to bronchial provocations with allergen, aspirin, leukotriene D_4, and histamine in asthmatics. *Am. Rev. Respir. Dis.* 1992; **146**: 96–103.
12   Drazen JM, O'Brien J, Sparrow D et al. Recovery of leukotriene E_4 from the urine of patients with airway obstruction. *Am. Rev. Respir. Dis.* 1992; **146**: 104–8.
13   Yoshida S, Sakamoto H, Ishizaki Y et al. Efficacy of leukotriene receptor antagonist in bronchial hyper-responsiveness and hypersensitivity to analgesic in aspirin-intolerant asthma. *Clin. Exp. Allergy* 2000; **30**: 64–70.
14   Sala A, Voelkel N, Maclouf J, Murphy RC. Leukotriene E_4 elimination and metabolism in normal human subjects. *J. Biol. Chem.* 1990; **265**: 21 771–8.
15   Lupinetti MD, Sheller JR, Catella F, Fitzgerald GA. Thromboxane biosynthesis in allergen-induced bronchospasm. Evidence for platelet activation. *Am. Rev. Respir. Dis.* 1989; **140**: 932–5.
16   Riutta A, Mucha I, Vapaatalo H. Solid-phase extraction of urinary 11-dehydrothromboxane B_2 for reliable determination with radioimmunoassay. *Anal. Biochem.* 1992; **202**: 299–305.
17   Christie PE, Tagari P, Ford-Hutchinson AW et al. Increased urinary LTE_4 excretion following inhalation of LTC_4 and LTE_4 in asthmatic subjects. *Eur. Respir. J.* 1994; **7**: 907–13.
18   Oosaki R, Mizushima Y, Kawasaki A et al. Fundamental studies on the measurement of urinary leukotriene E_4. *Arerugi* 1994; **43**: 127–33 (in Japanese).
19   Sheffer AL. International concensus report on diagnosis and treatment of asthma. *Clin. Exp. Allergy* 1992; **22**: 1–72.
20   Oosaki R, Mizushima Y, Kawasaki A et al. Urinary excretion of leukotriene E_4 and 11-dehydrothromboxane B_2 in patients with spontaneous asthma attacks. *Int. Arch. Allergy Immunol.* 1997; **114**: 373–8.
21   Osamura T, Mizuta R, Yoshioka H, Kawano K. Measurement of urinary 11-dehydro-thromboxane B_2 and 2,3-dinor-6-keto-prostaglandin $F_{1\alpha}$ levels in normal Japanese children. *Enshyo* 1996; **16**: 43–5 (in Japanese).
22   Bousquet J, Chanez P, Lacoste JY et al. Eosinophilic inflammation in asthma. *N. Engl. J. Med.* 1990; **323**: 1033–9.

Molecular analysis of B-cell differentiation in selective or partial IgA deficiency

T. ASANO*, H. KANEKO*, T. TERADA*, Y. KASAHARA*, T. FUKAO*, K. KASAHARA* & N. KONDO* *Department of Paediatrics, Gifu University School of Medicine, 40 Tsukasa-machi, Gifu 500–8705, Japan

SUMMARY

Selective IgA deficiency is the most common form of primary immunodeficiency, the molecular basis of which is unknown. To investigate the cause of selective IgA deficiency, we examined what stage of B-cell differentiation was blocked. DNA and RNA were extracted from three Japanese patients with selective IgA deficiency and three with a partial IgA deficiency. In selective IgA deficiency patients, Iα germline transcript expression levels decreased and α circle transcripts were not detected. Stimulation with PMA and TGF-β1 up-regulated Iα germline and α circle transcripts. In some patients, IgA secretion was induced by stimulation with anti-CD40, IL-4 and IL-10. In partial IgA deficiency patients, Iα germline, α circle transcripts and Cα mature transcripts were detected in the absence of stimulation. Our findings suggest that the decreased expression level of Iα germline transcripts before a class switch might be critical for the pathogenesis of some patients with selective IgA deficiency. However, in patients with a partial IgA deficiency, B-cell differentiation might be disturbed after a class switch.

Keywords selective IgA deficiency partial IgA deficiency germline transcripts circle transcripts TGF-β1

INTRODUCTION

Selective IgA deficiency is a common form of primary immuno-deficiency in Caucasians. However, there is a difference in frequency between the Caucasian and Asian populations (approximately 1 in 700 Caucasians and 1 in 18 500 Japanese being affected) [1,2]. Some IgA deficiency individuals have increased susceptibility to upper respiratory tract or gastrointestinal infections. Although the frequency of IgA deficiency is relatively high, the molecular basis of this disease is unknown and it is sometimes associated with deficiency of the IgG subclass or IgE and with common variable immunodeficiency [3–5]. Some IgG subclass deficiencies are caused by CH-gene deletions [6–8]. In addition, some cases of secondary IgA deficiency are caused by antiepileptic drugs [9], the others being associated with auto-immune disorders and malignancy. In patients with partial IgA deficiency whose serum IgA level is 2SD below normal levels [10], the serum IgA level increases with age. Therefore, it is conceivable that the mechanism underlying the IgA deficiency pathogenesis is heterogeneous [11].

B cells differentiate to IgA-bearing cells through a DNA recombination process that joins the Sμ to the Sα region with a deletion of the intervening sequence and this process is initiated by Iα germline transcripts. After switching, B cells normally differentiate from membrane IgA-bearing to IgA-secreting cells. The IgA deficiency may result from a defect or blockade at several levels, such as: 1) a structural gene defect; 2) impaired switching, which may be due to the lack of a specific switch recombinase, activation-induced cytidine deaminase (AID) [12], polymorphism, or accessibility of the S or I region; 3) failure of IgA-bearing B cells to differentiate into plasma cells; and 4) a defect at the transcriptional and/or at the post-transcriptional level [13]. There is an Sμ/Sα fragment or Sα/Sμ fragment of circular DNA in the IgA class switch recombination (CSR). Recently, Kinoshita et al. [14] examined whether isotype-specific transcripts are generated from I promoters located on excised circular DNA and found that isotype-specific I-Cμ transcripts, termed circle transcripts, were produced only in cells that express AID and undergo CSR in mice. Kinetic analysis of circle transcripts showed that they disappeared more quickly after the removal of cytokine stimulation than germline transcripts, circular DNA, or AID expression. Thus, circle transcripts are a hallmark of active CSR. In this study, to investigate the pathogenesis of IgA deficiency, we examined what stage of B-cell differentiation was blocked in this protein deficiency.

METHODS

Patients

Patients 1, 2 and 3 had a primary selective IgA deficiency whose serum IgA level was below the detection limit; patients 4, 5 and 6

Correspondence: Dr Tsutomu Asano 40 Tsukasa-machi, Gifu 500–8705, Japan.

E-mail: ben2@cc.gifu-u.ac.jp

had a partial IgA deficiency whose serum IgA level was above 5 mg/dL but 2SD below normal levels [10] at more than one year old, as shown in Table 1. Informed consent was obtained from all these patients or their parents.

Cell preparation and culture

Peripheral blood mononuclear cells (PBMCs) were isolated from the heparinized blood of patients and control donors by gradient centrifugation in Ficoll-Paque (Amersham Bioscience, Uppsala, Sweden) [16]. PBMCs were suspended at a density of 10^6/ml in an RPMI 1640 medium supplemented with 10% heat-inactivated fetal calf serum, L-glutamin (2 mmol/l), penicillin (100 U/ml) and streptomycin (100μg/ml). PBMCs (10^6/ml) were cultured in the presence or absence of phorbol myristate acetate (PMA) (10 ng/ml) (Sigma Aldrich, St. Louis, MO, USA) and recombinant human-TGF-β1 (1 ng/ml) (R & D systems, Inc., Wiesbaden, Germany) for 24 h. Further, PBMCs obtained from patients of the selective IgA deficiency were cultured in the presence or absence of anti-CD40, IL-4 and IL-10 for seven days.

DNA transfer blot analysis and sequencing of IgA constant region

Genomic DNA was purified from a polynuclear cell fraction with a Sepa Gene (Sanko Jyunyaku, Tokyo, Japan). DNA transfer blot analysis was performed according to a previous report using a Cα 2 probe, which was a 2-kb Pst I fragment from ch. h. Igα–25 [17].

The fragments of the I promoter region, exon1, exon2, exon3 and the membrane exon of the α1 gene were amplified, ligated to a T-vector (Novagen, Madison, WI, USA) and sequenced using an ABI 377 DNA Sequencing System (Applied Biosystems, Indianapolis, IN, USA).

PCR amplification of α 1 hs1, 2 enhancer

DNA fragments, including the region of variable number of tandem repeats (VNTR), of the α 1 hs1, 2 enhancer were amplified with consensus-flanking primers and the cycling conditions were as follows: sense 5′-GGGTCCTGGTCCCAAAGATGGC-3′ and antisense 5′-TTCCCAGGGGTCCTGTGGGTCC-3′ [18]; 94°C for 1 min, 64°C for 1 min and 72°C for 1 min for 40 cycles.

cDNA synthesis

RNA was extracted from PBMCs cultured in the presence or absence of PMA and TGF-β1 for 24 h using an Isogen kit (Nippon Gene, Tokyo, Japan) and cDNA synthesis from 2μg of RNA was performed using a cDNA synthesis kit according to the manufacturer's instructions.

Semiquantitative PCR analysis of Iα germline transcripts

Figure 1 schematically shows the locations of oligomers used in the following experiments in the regions of JH, Iα 1, Cα 1 and Cμ. PCR amplification of the Iα germline transcripts was carried out using the primers and cycling conditions as follows. The sense primer was chosen from the 3′ region of the Iα 1 exon and the antisense primer was obtained from the 3′ region of the Cα 1 exon1 [19]. The following primers were used: IS, sense 5′-TGAGTGGACCTGCCATGA-3′(GenBank accession number-L04540), CA1, antisense 5′-CTGGGATTCGTGTAGT GCTT-3′ (J00220) (Fig. 1). For unstimulated cDNA; 94°C for 1 min, 58°C for 1 min and 72°C for 1 min for 28, 32, 36, 40 cycles. For stimulated cDNA; 94°C for 1 min, 58°C for 1 min and 72°C for 1 min for 35 cycles. The plasmid containing a 337 bp cDNA fragment from Iα germline transcripts was partially substituted with a 267 bp fragment from BLM cDNA [20] and was used as a competitor DNA. The PCR product of the wild type was 337 bp and that of the competitor was 287 bp. Each template contained 1μl of cDNA from 2μg of RNA extracted from PBMCs cultured in the presence of PMA and TGF-β1 and one of fivefold dilutions of the competitor DNA.

## Nested PCR analysis of α circle transcripts

Nested PCR analysis of α circle transcripts was carried out using the primers and cycling conditions as follows. The sense primer was chosen from the 3′ region of the Iα 1 exon and the antisense primer was obtained from the 3′ region of the Cμ. In the first round, the primers P1 and P4 were used at 95°C for 9 min in the denaturing step, 95°C for 1 min, 51°C for 1 min and 72°C for 2 min for 35 cycles. In the second round, the primers P2 (IS) and P3 were used at 94°C for 1 min, 58°C for 1 min and 72°C for 1 min for 35 cycles. The primers were: P1, 5′-CACAGCCAGC

Table 1. Immunlogical data of patients

Patient no.	Sex	Age	Serum Ig (mg/dl)†			Surface Ig-bearing B cells (%)			IgG subclass (mg/dl)			
			IgG	IgA	IgM	IgG	IgA	IgM	IgG1	IgG2	IgG3	IgG4
Selective IgA deficiency												
1	M	6 years	1120 (630–1490)	<5 (45–258)	110 (72–305)	1	0	23	619	255	57·3	33·9
2	F	14 years	1750 (760–1680)	<5 (77–371)	259 (69–296)	1	1	13	630	625	35·1	18·4
3	F	7 years	1430 (660–1340)	<5 (51–279)	104 (73–310)	0	0	5	893	382	47·4	59·4
Partial IgA deficiency												
4	M	21 months	889 (460–1220)	13 (16–128)	69 (57–260)	1	1	3	466	98.4	13·5	16·2
5	F	16 months	465 (460–1220)	9 (16–128)	70 (57–260)	1	0	5	306	69.3	27·6	3·8
6	M	18 months	474 (460–1220)	10 (16–128)	83 (57–260)	2	0	11	295	97.0	40·0	4·4

†Normal range (2·5–97·5 percentile) of serum Ig are given in brackets where appropriate; they are from *Normal Range for Clinical Testing of Japanese Children* [15].
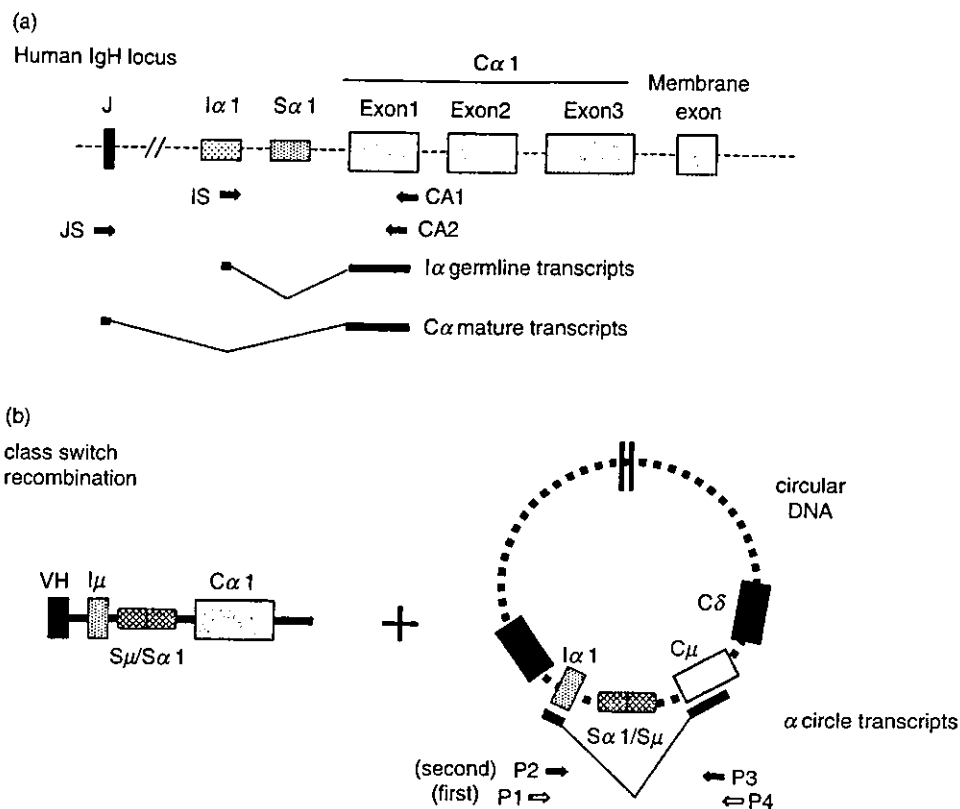
Fig. 1. (a) Schematic of PCR strategies. The human IgH locus after VDJ rearrangement is shown schematically at the top. Primers are indicated by arrows. The PCR fragments amplified from cDNA are indicated by thick lines with a V-shaped line representing splicing. (b) Schematic of PCR strategies for circle transcripts. The IgA class switch recombination is shown. Thick lines below circular DNA indicate exons of α circle transcripts connected with a V-shaped line representing splicing.

GAGGCAGAGC-3' (L04540), P2, 5'-TGAGTGGACCTGC CATGA-3' (L04540), P3, 5'-CGTCTGTGCCTGCATGACG-3' (X14940), P4, 5'-ACGAAGACGCTCACTTTGGG-3' (X14940) (Fig. 1).

PCR analysis of Cα mature transcripts

PCR amplification of Cα mature transcripts was carried out using the primers and cycling conditions as follows. The JH consensus sequence was used as the sense primer and the antisense primer was obtained from the 3' region of the Cα 1 exon1. The following primers were used: JS, sense 5'-CCTGGTCAC CGTCTCCTCA-3' (L20778), CA2, antisense 5'-ACGTGGCAT GTCACGGACTT-3' (J00220) (Fig. 1); 94°C for 1 min, 59°C for 1min and 72°C for 1 min for 32, 34, 36 and 38 cycles.

Assay of IgA secretion

The concentration of IgA in the supernatant of PBMCs cultured in the presence or absence of anti-CD40, IL-4 and IL-10 for seven days was assayed by an enzyme-linked immunosorbent assay kit (Cygnus Technologies, Southport, NC, USA).

RESULTS

Southern blot analysis of Cα constant region

PstI-digested DNA samples from the six patients and one control subject were analysed using a Cα2 gene probe. Human Cα genes are sufficiently homologous and detect both Cα1 and Cα2 genes.

As shown in Fig. 2a, the large deletion of the constant region on the Cα genes was not detected in all subjects.

Genome sequence of Cα constant region

To examine the mutation of the α heavy chain, PCR analysis was performed using the primers of the I promoter region, exon1, exon2, exon3 and the membrane exon of the α1 gene. There were no mutations in these regions. The polymorphism of the Cα 1 gene 882G→C (E175D) in exon2 was detected in patients 1, 3 and 5.

PCR amplification of α1 hs1, 2 enhancer

We analysed the α hs1, 2 enhancer, which strongly regulates human IgH expression and is located within 12 kb downstream of both the human Ig Cα 1 and Cα 2 genes [18,21]. The α 1 hs1, 2 enhancer is located between Cα 1 and φ γ (Fig. 2b). As shown in Fig. 2c, a fragment of the α 1 hs1, 2 enhancer was detected in all subjects. α 1 hs1, 2 has three variants with VNTR, namely α 1 A, α1B and α1C (including one, two and three repeats, respectively) [18]. The sizes of the PCR products were 462 bp, 515 bp and 568 bp for α 1 A, α 1 B and α 1 C, respectively. Controls 1 and 2, patients 2, 3 and 4 had the α 1 A/A allele, patient 1 had α 1B/C, patient 5 had α 1 A/B and patient 6 had α 1 A/C.

Germline transcript expression in IgA deficiency

Germline transcripts are indispensable for the initiation of CSR. We examined the expression of Iα germline transcripts using a

(a)

(b)

(c)
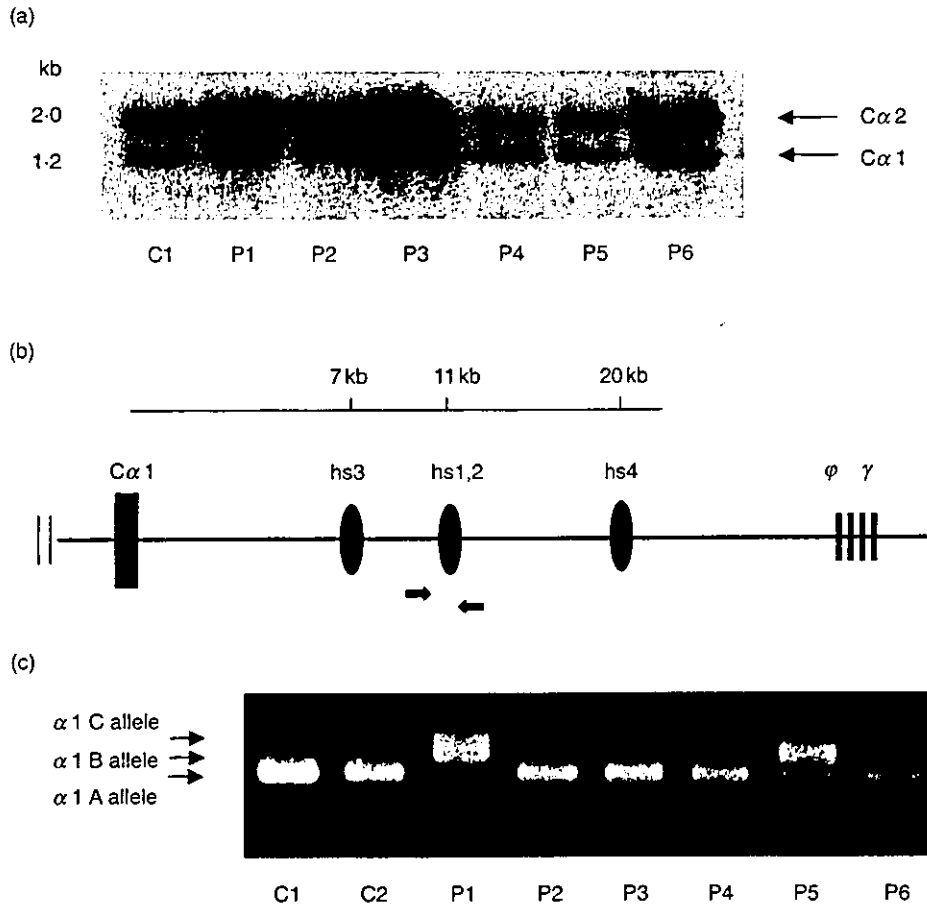
Fig. 2. (a) Cα gene hybridization pattern. PstI-digested DNA samples from control (C1) and patients (P1–P6) were analysed by Southern blot analysis. The probe was a 2-kb Cα2 fragment. The length in kb of each Cα gene, is indicated. (b) Schematic of PCR strategies for the detection of α1 hs1,2 enhancer located between Cα1 and φγ. The α1 hs3, α1 hs1,2, and α1 hs4 fragments are located 7, 11, and 20kb downstream of the Cα1 gene, respectively (20). Primers are indicated by arrows. (c) PCR fragments of α1 hs1,2 enhancer from genome DNA are shown. PCR products of sizes 462 bp, 515 bp and 568 bp for α1 A, α1 B and α1 C, respectively. C1 and C2, normal controls; P1–P6, patients 1–6.

semiquantitative PCR analysis. First, the expression of the Iα germline transcripts of unstimulated PBMCs was examined by RT-PCR using different cycles and that expression from patients 1, 2 and 3 was not clearly detected even after 40 cycles were run and the expression levels were markedly lower than those in controls. In patients 4, 5 and 6, the expression levels were slightly lower than those in controls but the Iα germline transcripts were detected at significant levels (Fig. 3a). Next, competitive PCR analysis was applied to measure the expression level of Iα germline transcripts of PBMCs stimulated by PMA and TGF-β1. In both controls and IgA deficiency patients, the target cDNA and competitor were almost equivalent between lane 3 and lane 4 (Fig. 3b). The Iα germline transcripts of PBMCs from the selective and partial IgA deficiency patients were induced by PMA and TGF-β1 at a level almost equal to those in controls. The Iα germline transcripts of PBMCs from the selective and partial IgA deficiency patients were induced by PMA and TGF-β1 at a level almost equal to those in controls.

Circle transcript expression in IgA deficiency
To determine whether the CSR from IgM to IgA could occur in the IgA deficiency patients, the expression of the α circle transcripts was examined. The α circle transcripts were generated

from Iα promoters located on excised circular DNA and Cμ (Fig. 1b). Because the circle transcripts were not clearly detected at first PCR (data not shown) even in controls, we performed nested PCR and the α circle transcripts were detected in controls, patients 4, 5 and 6, but not in patients 1, 2 and 3 (Fig. 4). However, the circle transcripts were induced in PBMCs from patients 1, 2 and 3 after stimulation with PMA and TGF-β1.

Mature transcript expression in IgA deficiency
We further examined the expression of Cα mature transcripts, including both their membrane and secreted forms, by RT-PCR using different cycles. As shown in Fig. 5a, the expression levels of the Cα mature transcripts of unstimulated PBMCs from patients 1, 2, 3 and 4 decreased. In patients 5 and 6, the expression levels of the Cα mature transcripts decreased slightly compared to controls. The Cα mature transcripts were induced by PMA and TGF-β1 in patients 1 and 2. In patient 3, the Cα mature transcripts were not markedly induced by PMA and TGF-β1 stimulation (Fig. 5b).

IgA secretion induced by anti-CD40, IL-4 and IL-10
IgA secretion by CD40-activated PBMCs from patients with the selective IgA deficiency was examined. Anti-CD40, IL-4 and

(a) Unstimulated

(b) PMA and TGF-β1 stimulated
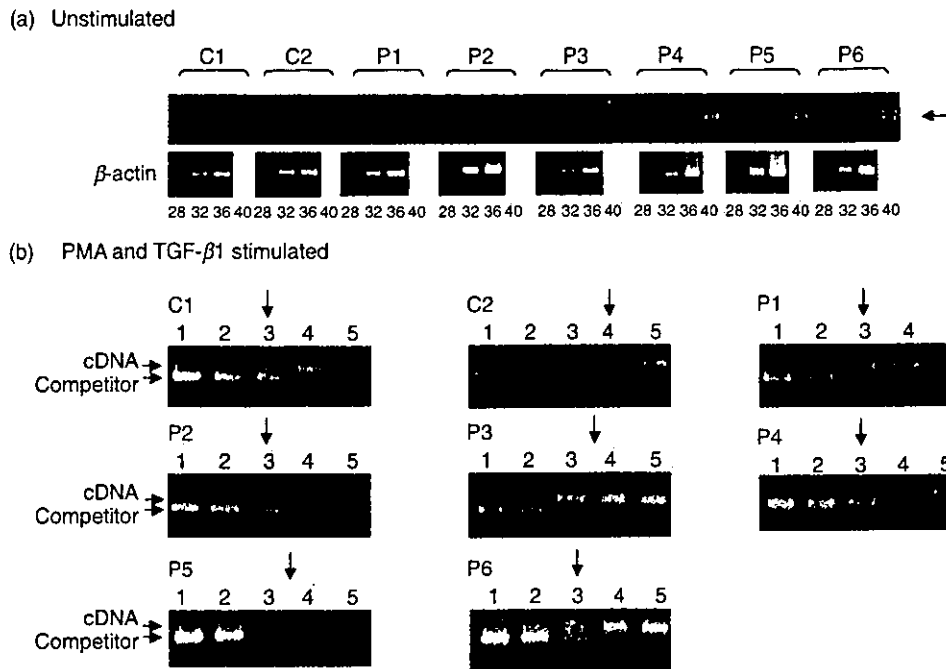
Fig. 3. (a) Expression of Iα germline transcripts in unstimulated PBMCs. Semiquantitative determination using RT-PCR analysis. In each case, 28, 32, 36 and 40 cycles were run. β-actin was used as a control with a run of 28, 32 and 36 cycles. The position of target cDNA is indicated by an arrow. C1 and C2, normal controls; P1–P6, patients 1–6. (b) Competitive PCR of the expression of Iα germline transcripts. Each template contained the same amount of cDNA synthesized from RNA extracted from PBMCs after stimulation with PMA and TGF-β1 and one of fivefold dilutions of Iα germline transcript competitor (lanes 1–5). Each equivalent point is indicated by an arrow. C1 and C2, normal controls; P1–P6, patients 1–6.

(a) Unstimulated

(b) PMA and TGF-β1 stimulated
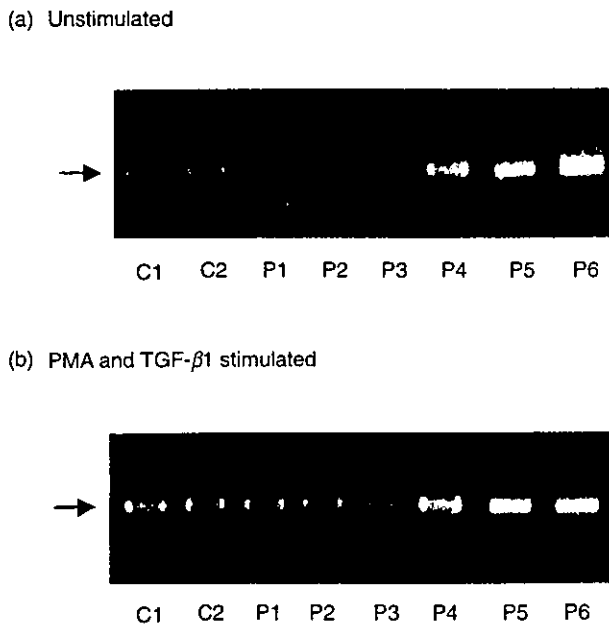
Fig. 4. Detection of α circle transcripts in PBMCs cultured without or with PMA and TGF-β1. The second PCR fragments of α circle transcripts are shown and are indicated by arrows. C1 and C2, normal controls; P1–P6, patients 1–6.

IL-10 induced IgA secretion in PBMCs from control and patient 1. In patient 2, IgA secretion was slightly induced. However, in patient 3, it was not induced by the same stimulation (Fig. 5c).

DISCUSSION

In this study, we demonstrated the following in selective IgA deficiency patients: 1) Cα genes were not deleted; 2) expression levels of Iα germline transcripts of unstimulated PBMCs markedly decreased; 3) Iα germline transcripts were induced by PMA and TGF-β1; 4) α circle transcripts of unstimulated PBMCs were not detected; 5) α circle transcripts were detected after stimulation; 6) Cα mature transcripts were induced by PMA and TGF-β1; and 7) IgA secretion was induced by appropriate stimulation.

Thus, the decreased expression level of the Iα germline transcripts is critical for the pathogenesis of the selective IgA deficiency in our patients and it is possible to induce IgA CSR in these patients. In partial IgA deficiency patients, although the expression levels of the Iα germline transcripts were slightly lower than controls, α circle and mature transcripts were detected. The number of surface IgA-bearing B cells was low in all of the IgA deficiency patients. It is suggested that a defect of the membrane-bound IgA at the post-transcriptional level may cause low IgA production in partial IgA deficiency patients. The expression of the membrane-bound immunoglobulin is indispensable for the generation of efficient primary and secondary immunoglobulin responses [22]. In this study, there was no mutation of the alternative splice site for the membrane exon of the Cα1 gene.

The Iα germline transcripts are conceivably critical for the initiation of switching from Cμ to Cα. In a previous study, it was reported that the Iα germline transcripts were absent in peripheral B cells of IgA deficiency patients, suggesting the impairment of IgA switching [13]. However, it was also reported that the Iα germline transcripts were detected in all of the IgA deficiency patients tested as well as in normal controls [23]. Consistent with

(a) Unstimulated

(b) PMA and TGF-β1 stimulated

(c)
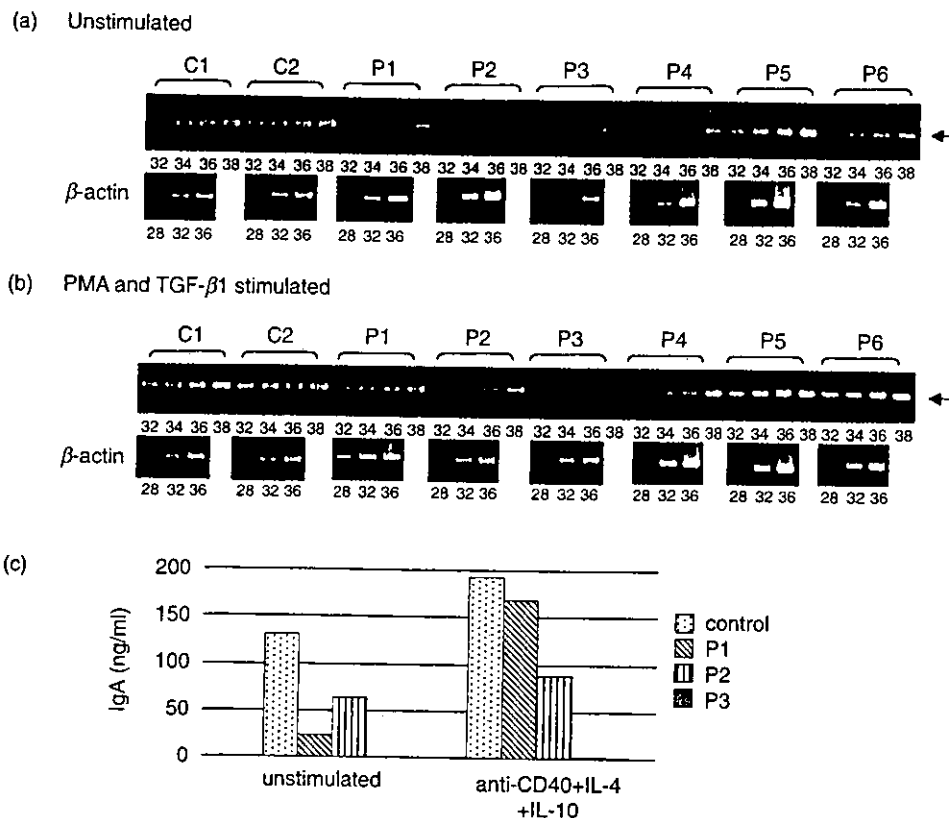
Fig. 5. Expression of Cα mature transcripts in PBMCs cultured without (a) or with (b) PMA and TGF-β1. Semiquantitative determination using RT-PCR analysis. In each case, 32, 34, 36 and 38 cycles were run. β-actin was used as a control with a run of 28, 32 and 36 cycles. The positions of target cDNA are indicated by arrows. C1 and C2, normal controls; P1–P6, patients 1–6. (c) IgA secretion was induced by activation of PBMCs. PBMCs (10^6/mL) were cultured in the presence or absence of anti-CD40, IL-4, and IL-10 for seven days. Concentration of IgA in the supernatant of PBMCs was measured by an enzyme-linked immunosorbent assay. P1–P3, patients 1–3.

previous reports, our study revealed two different types of defects in B-cell differentiation – one was a decreased Cα mRNA level in IgA-switched B cells and the other was a switching defect, which may be present in IgA deficiency patients.

It is possible that some stimulation corresponding to that with PMA and TGF-β1 is reduced or blocked in selective IgA deficiency patients. In patients 1 and 2 but not 3, PMA and TGF-β1 could induced the α germline and mature transcripts and CD40 and appropriate cytokines induced IgA production. Therefore, in patient 3, the PMA and TGF-β1 pathways might be blocked, which were common signals in CD40 and cytokines, such as mitogen-activated protein kinase [24,25] and protein kinase C [26] signal transduction. In patient 1 and 2, distinct signal pathways between TGF-β1 and CD40 might be disturbed in B cells. Muller *et al.* reported that the serum levels of TGF-β1 in IgA deficiency patients were low [27]. In our cases, there was no difference in the level of TGF-β1 in plasma among selective IgA deficiency patients, partial IgA deficiency patients and controls (data not shown).

In recent studies, many lines of evidence have been presented indicating that primary IgA deficiency is inherited and associated with a certain major histocompatibility complex-conserved haplotype mainly in populations of the western world [28–30]. However, there are only a few studies that show an association of haplotypes, such as [HLA-A1, B8, DR3] [30], with the IgA deficiency in Japanese patients [31]. In our study, the decreased

expression level of the Iα germline transcripts is critical for the pathogenesis of the selective IgA deficiency in some patients. Partial IgA deficiency has distinct causes from those of the selective IgA deficiency. Since in most of the partial IgA deficiency patients the serum IgA level normalizes with age, the existence of suppressor factors for IgA B-cell differentiation may be assumed. In our cases, B-cell differentiation in selective IgA deficiency patients showed impairment before the CSR stage, while B-cell differentiation in partial IgA deficiency patients showed impairment after the CSR stage.

REFERENCES

1 World Health Organisation. Primary immunodeficiency diseases. Report of a WHO scientific group. Clin Exp Immunol 1997; **109** (Suppl. 1):1–28.

2 Kanoh T, Mizumoto T, Yasuda N *et al.* Selective IgA Deficiency in Japanese Blood Donors: frequency and statistical analysis. Vox Sang 1986; **50**:81–6.

3 Espanol T, Catala M, Hernandez M, Caragol I, Bertran JM. Development of a common variable immunodeficiency in IgA deficient patients. Clin Immunol Immunopathol 1996; **80**:333–5.

4 Johnson ML, Keeton LG, Zhu ZB, Volanakis JE, Cooper MD, Schroeder JR. Age-related changes in serum immunoglobulins in patients with familial IgA deficiency and common variable immunodeficiency (CVID). Clin Exp Immunol 1997; **108**:477–83.

5 Seligmann M, Aucouturier P, Danon F, Preudhomme JL. Changes in serum immunogulobulin patterns in adults with common variable immunodeficiency. Clin Exp Immunol 1991; 84:23–7.

6 Bottaro A, de Marchi M, de Lange GG, Carbonara AO. Gene deletions in the human immunoglobulin heavy chain constant region gene cluster. Exp Clin Immunogenet 1989; 6:55–9.

7 Lefranc MP, Hammarstrom L, Smith CI, Lefranc G. Gene deletions in the human immunoglobulin heavy chain constant region locus: molecular and immunological analysis. Immunodefic Rev 1991; 2:265–81.

8 Terada T, Kaneko H, Li A, Kasahara K, Ibe M, Yokota S, Kondo N. Analysis of Ig subclass deficiency: First reported case of IgG2, IgG4, and IgA deficiency caused by deletion of $C\alpha$ 1, $\varphi C\gamma$, $C\gamma$2, $C\gamma$4, and $C\varepsilon$ in a Mongoloid patient. J Allergy Clin Immunol 2001; 108:602–6.

9 Maeoka Y, Hara T, Dejima S, Takeshita K. IgA and IgG2 deficiency associated with zonisamide therapy: a case report. Epilepsia 1997; 38:611–3.

10 Nagao AT, Mai FH, Pereira AB, Carnerio-Sampaio MMS. Measurement of salivary, urinary and fecal secretory IgA levels in children with partial or total IgA deficiency. J Invest Allergol Clin Immunol 1994; 4:234–7.

11 Burrows PD, Cooper MD. Iga Deficiency Adv Immunol 1997; 65:245–76.

12 Arakawa H, Hauschild J, Buerstedde JM. Requirement of the activation-induced deaminase (AID) gene for immunoglobulin gene conversion. Science 2002; 295:1301–6.

13 Islam KB, Baskin B, Nilsson L, Hammarstom L, Sideras P, Smith CIE. Molecular analysis of IgA deficiency. Evidence for impaired switching to IgA. J Immunol 1994; 152:1442–52.

14 Kinoshita K, Harigai M, Fagarasan S, Muramatsu M, Honjo T. A hallmark of active class switch recombination: Transcripts directed by I promoters on looped-out circular DNAs. Proc Natl Acad Sci USA 2001; 98:12620–3.

15 The study team for the normal range of children. Normal range for clinical testing of Japanese children. Tokyo: Japan Public Health Association 1996:263–78. (in Japanese).

16 Kondo N, Fukutomi O, Agata H *et al*. The role of T lymphocytes in patients with food-sensitive atopic dermatitis. J Allergy Clin Immunol 1993; 91:658–68.

17 Kaneko H, Kondo N, Motoyoshi F, Mori Y, Kobayashi Y, Ozawa T, Orii T. Expression of the alpha-chain gene in heterogeneous IgA immunodeficiency. Scand J Immunol 1990; 32:483–9.

18 Denizot Y, Pinaud E, Aupetit C, Morvan CL, Magnoux E, Aldigier JC, Cogne M. Polymorphism of the human α 1 immunoglobulin gene 3′ enhancer hs1,2 and its relation to gene expression. Immunology 2001; 103:35–40.

19 Nilsson L, Islam KB, Olafsson O, Zalcberg I, Samakovlis C, Hammarstrom L, Smith CIE, Sideras P. Structure of TGF-β1-induced human immunoglobulin $C\alpha$ 1 and $C\alpha$ 2 germ-line transcripts. Int Immunol 1991; 3:1107–15.

20 Ellis NA, Groden JYeTZ, Straughen J, Lennon DJ, Ciocci S, Proytcheva M, German J. The Bloom's syndrome gene product is homologous to RecQ helicases. Cell 1995; 83:655–66.

21 Hu Y, Pan Q, Pardali E, Mills FC, Bernestein RM, Max EE, Sideras P, Hammarstrom L. Regulation of germline promoters by the two human Ig heavy chain 3′α enhancers. J Immunol 2000; 164:6380–6.

22 Tashita H, Fukao T, Kaneko H, Teramoto T, Inoue R, Kasahara K, Kondo N. Molecular basis of selective IgG2 deficiency. The mutated membrane-bound form of γ 2 heavy chain caused complete IgG2 deficiency in two Japanese sibilings. J Clin Invest 1998; 101:677–81.

23 Wang Z, Yunis D, Irigoyen M, Kitchens B, Bottaro A, Alt FW, Alper CA. Discordance between IgA switching at the DNA level and IgA expression at the mRNA level in IgA-deficient patients. Clin Immunol 1999; 91 (3):263–70.

24 Zhang K, Zhang L, Zhu D, Bae D, Nel A, Saxon A. CD40-mediated p38 mitogen-activated protein kinase activation is required for immunoglobulin class switch recombination to IgE. J Allergy Clin Immunol 2002; 110:421–8.

25 Yamaguchi K, Shirakabe K, Shibuya H *et al*. Identification of a member of the MAPKKK family as a potential mediator of TGFβ signal transduction. Science 1995; 270:2008–11.

26 Yan JC, Wu ZG, Kong XT, Zong RQ, Zhan LZ. Effect of CD40–CD40 ligand interaction on diacylglycerol-protein kinase C and inositol triphosphate- Ca^{2+} signal transduction pathway in human umbilical vein endothelial cells. Clin Chim Acta 2003; 337:133–40.

27 Muller F, Aukrust P, Nilssen DE, Froland SS. Reduced serum level of transforming growth factor-β in patients with IgA deficiency. Clin Immunol Immunopathol 1995; 76:203–8.

28 Vorechovsky I, Webster ADB, Plebani A, Hammarstrom L. Genetic linkage of IgA deficiency to the major histocompatibility complex: evidence for allele segregation distortion, parent-of-origin penetrance differences and the role of anti-IgA antibodies in disease predisposition. Am J Hum Genet 1999; 64:1096–109.

29 Kralovicova J, Hammarstrom L, Plebani A, Webster ADB, Vorechovsky I. Fine-scale mapping at IGAD1 and genome-wide genetic linkage analysis implicate HLA-DQ/DR as a major susceptibility locus in selective IgA deficiency and common variable immunodeficiency. J Immunol 2003; 170:2765–75.

30 Price P, Witt C, Allcock R *et al*. The genetic basis for the association of the 8.1 ancestral haplotype (A1,B8,DR3) with multiple immunopathological diseases. Immunol Rev 1999; 167: 257–74.

31 Futakami Y, Suto K, Onodera Y *et al*. HLA antigen in Japanese blood donors with IgA deficiency. Jp J Transfus Med 2002; 48:298–03. (in Japanese).

ELSEVIER

Peroxisomal localization in the developing mouse cerebellum: implications for neuronal abnormalities related to deficiencies in peroxisomes

Tomoko Nagase[a,*], Nobuyuki Shimozawa[a], Yasuhiko Takemoto[a], Yasuyuki Suzuki[b], Masayuki Komori[c], Naomi Kondo[a]

[a]*Department of Pediatrics, Gifu University School of Medicine, 40 Tsukasa-machi, Gifu 500-8705, Japan*
[b]*Medical Education Development Center, Gifu University School of Medicine, 40 Tsukasa-machi, Gifu 500-8705, Japan*
[c]*Laboratory of Cellular and Molecular Biology, Department of Veterinary Science, Graduate School of Agriculture and Biological Sciences, Osaka Prefecture University, 1-1 Gakuen-cho, Sakai, Osaka 599-8531, Japan*

Abstract

In subjects with Zellweger syndrome, the most severe phenotype of peroxisomal biogenesis disorder, brain abnormalities include cortical dysplasia, neuronal heterotopia, and dysmyelination. To clarify the relationship between the lack of peroxisomes and neuronal abnormalities, we investigated peroxisomal localization in the mouse cerebellum, using double immunofluorescent staining for peroxisomal proteins.

On immunostaining for peroxisomal matrix protein, while there are few peroxisomes in Purkinje cells, many locate in astroglia, especially soma of Bergmann glia. Clusters of peroxisomes were seen on the inferior side of the Purkinje cell layer in mice on postnatal days 3–5, and with time there was a shift to the superior side. The peroxisomal punctate pattern was seen to be radial and co-localized with Bergmann glial fibers. In cultured cells from the mouse cerebellum, peroxisomes were few in Purkinje cells, whereas many were evident in glial fibrillary acidic protein-positive cells. On the other hand, on immunostaining for peroxisomal membrane protein Pex14p, many particles were seen in Purkinje cells during all developmental stages, which means Purkinje cells possessed empty peroxisomal structures similar to findings of fibroblasts from the Zellweger patients. As peroxisomes in glial cells may control the development of neurons, the neuron–glial interaction and mechanisms of developing central nervous systems deserve ongoing attention.
© 2004 Elsevier B.V. All rights reserved.

Keywords: Peroxisome; Purkinje cell; Glia; Mouse; Cerebellum; Development

1. Introduction

Peroxisomes are single-membrane lined organelles present in virtually all eukaryotic cells. In most human cells, their abundance ranges from less than a hundred to more than a thousand per cell. The granular matrix of the organelle contains more than 50 matrix enzymes that participate in a wide variety of metabolic pathways, including beta-oxidation of certain fatty acids and biosynthesis of ether phospholipids, bile acids, and isoprene compounds. Peroxisome biogenesis disorders (PBDs) are caused by defects in PEX genes involved in import of peroxisome matrix proteins and biosynthesis of peroxisomal membrane proteins. PBDs constitute a group of progressive neurologic diseases and onset and severity can vary [1,2]. Neuropathologic lesions are of three major classes: abnormalities in neuronal migration or differentiation, defects in the formation or maintenance of central white matter, and post-developmental neuronal degenerations [3]. We identified the first known pathologic gene in 1992 [4], and enormous progress in defining gene defects has been achieved. Nevertheless, the molecular mechanisms underlying the pathogenesis have remained an open question. To clarify potential links between the peroxisome and the mechanisms related to neuronal abnormalities, we investigated the localization of peroxisomes in the cerebellum of the mouse during developmental stages.

* Corresponding author. Tel.: +81-58-267-2817; fax: +81-58-265-9011.
E-mail address: tomoko-n@cc.gifu-u.ac.jp (T. Nagase).

2. Materials and methods

The Institute of Cancer Research (ICR) mice of both sexes at different ages were used in the present study. The age groups studied were: embryonic day 15 (E15), postnatal days 0 (P0), P3, P5, P7, P10, P14 and P21. Mice were decapitated after administrating deep diethyl ether anesthesia to these mice. E15 mice were used in cell cultured studies, and mice on postnatal days were used in immunohistochemical studies, respectively. Animal handling, maintenance and experimentations were done in accordance with guidelines set by the Institutional Animal Care and Use Committee.

2.1. Immunohistochemistry

The obtained brains were immediately placed in liquid nitrogen, then frozen parasagittal sections (8 μm thick) were prepared on a cryostat and mounted on glass slides. Sections were fixed with 4% paraformaldehyde/0.1 M potassium phosphate buffer (pH 7.4) for 20 min then transferred to phosphate-buffered saline (PBS).

Sections were permeabilized with PBS containing 0.1% Triton X-100 for 30 min at room temperature (RT), then transferred to PBS containing 2% fetal calf serum (FCS) and 0.1% Triton X-100 for 1 h at RT for blocking. Sections were treated with anti-catalase rabbit antibody (a generous gift from Dr. T. Hashimoto, Shinshu University, Japan), anti-acyl-CoA oxidase (AOX) rabbit antibody, anti-D-bifunctional protein (D-BP) rabbit antibody, anti-peroxisomal 3-ketoacyl-CoA thiolase (PT) rabbit antibody (antibodies for AOX, D-BP and PT are generous gifts from Dr. N. Usuda, Fujita Health University, Aichi, Japan), anti-Pex14p rabbit antibody, anti-inositol 1,4,5 triphosphate receptor (IP3R) mouse antibody (a generous gift from Dr. K. Mikoshiba, The University of Tokyo, Japan), anti-vimentin goat antibody (Santa Cruz), and anti-glial fibrillary acidic protein (GFAP) mouse antibody (Chemicon). An anti-catalase antibody, anti-AOX antibody, anti-D-BP antibody and anti-PT antibody, which are for matrix enzymes, were used to analyze peroxisomes as markers of peroxisomes [5,6]. An anti-Pex14p antibody, a peroxisomal membrane protein was also used to analyze peroxisomal structures (Komori et al. unpublished data). An anti-IP3R antibody was used to confirm the identity of Purkinje cells [7]. Antibodies for vimentin (P0, P3 and P5) and GFAP (P7, P10 and P21), which are intermediate filaments, were used to analyze glial cells [8]. Primary antibody binding was detected by incubation with appropriate fluorescein-, Cy3-, or rhodamine-conjugated secondary antibodies. For observation we used a confocal laser-scanning microscope (LSM 5 PASCAL, Carl Zeiss). Images were processed using Adobe Photoshop 6.0 software.

2.2. Cell cultures

Cerebella of E15 mice were dissected, freed of meninges, collected in Hanks' Balanced Salt Solution (14175-095,

GIBCO) and kept on ice until digestion using a digestion kit (MB-X9901, SUMILON). Cells were maintained in 6-well culture plates (3516, costar) with a polyethyleneimine-coated coverslip and under serum-free conditions. Cells were plated at a density of 6×10^4 cells per cm^2. First, the cells were cultured with serum-free medium (MB-X9501, SUMILON), followed on days in vitro (DIV) 5 and 10, then all the medium was replaced with fresh medium (Neurobasal medium, 21103, GIBCO) supplemented with B27 supplement (2 ml of B27 50 × concentrate (17504, GIBCO) to 100 ml Neurobasal medium) and 0.5 mM L-glutamine. On DIV14, cells were fixed with 4% paraformaldehyde/0.1 M potassium phosphate buffer (pH 7.4) for 1 h and washed with PBS.

Cultured cells were permeabilized with PBS containing 0.1% Triton X-100 for 30 min at RT, then transferred to PBS containing 2% FCS and 0.1% Triton X-100 for 1 h at RT for blocking. These cells were treated with an anti-catalase rabbit antibody/Pex14p rabbit antibody, and anti-calbindin D-28 k mouse antibody (SIGMA)/GFAP mouse antibody. An anti-calbindin antibody was used to analyze the Purkinje cells [9]. Primary antibody binding was evident by incubation with appropriate fluorescein- or rhodamine-conjugated secondary antibodies. Observation and image processing were done as in the immunohistochemical studies.

3. Results

3.1. Immunohistochemistry

In immunohistochemical studies on the cerebellar sections, IP3R was predominantly expressed in Purkinje cells on all postnatal days tested, whereas in the P0 they were hardly detectable. Purkinje cells were lined, multi-layered, and formed an orderly single layer by P3. However, dendrites were hardly detectable in P0, and branches and extension increased towards the pia mater. In P21, dendrites spread into a reticular pattern in a molecular layer (Fig. 1A, D, G, J, M and P).

In P0–P3, peroxisomes detected with catalase antibody were seen in a diffuse punctate pattern. In P5, peroxisomes accumulated in the inferior of the Purkinje layer, where the locus shifted to a lateral form with time. After P10, the peroxisomal punctate patterns also run radially in the molecular layer. The peak was seen in P7–P10 (Fig. 1B, E, H, K, N and Q). Other peroxisomal matrix proteins, AOX (Fig. 3A, E, I, M, Q and U), D-BP (Fig. 3B, F, J, N, R and V), and PT (Fig. 3C, G, K, O, S and W) were expressed much like catalase however slightly more peroxisomes existed in Purkinje cells.

GFAP was expressed more extensively after P7, which means that the glial cells were immature in early postnatal days. The Bergmann glial fibers were elongated toward to the pia mater (Fig. 2A, D, G, J, M and P).
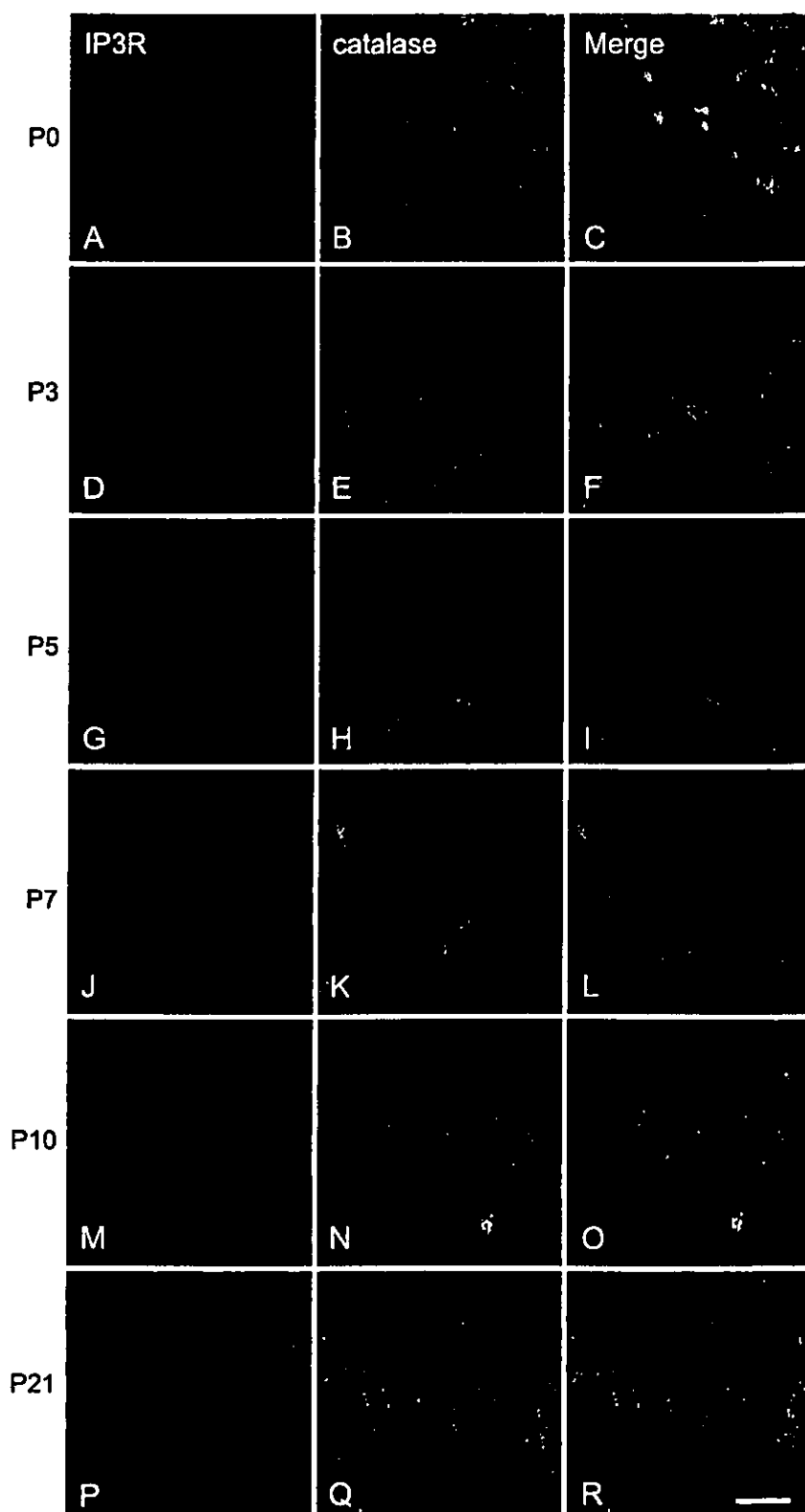
Fig. 1. Double immunofluorescence for IP3R (A, D, G, J, M and P) and catalase (B, E, H, K, N and Q) in the mouse cerebellar cortex on various postnatal days. All images were taken near the midpoint of the preculminate fissure. The complex pattern of catalase is evident in the inferior of the Purkinje layer in the early postnatal days (-P5), then becomes lateral. Note peroxisomes are hardly localized in Purkinje cells. Scale bar indicates 20 μm.
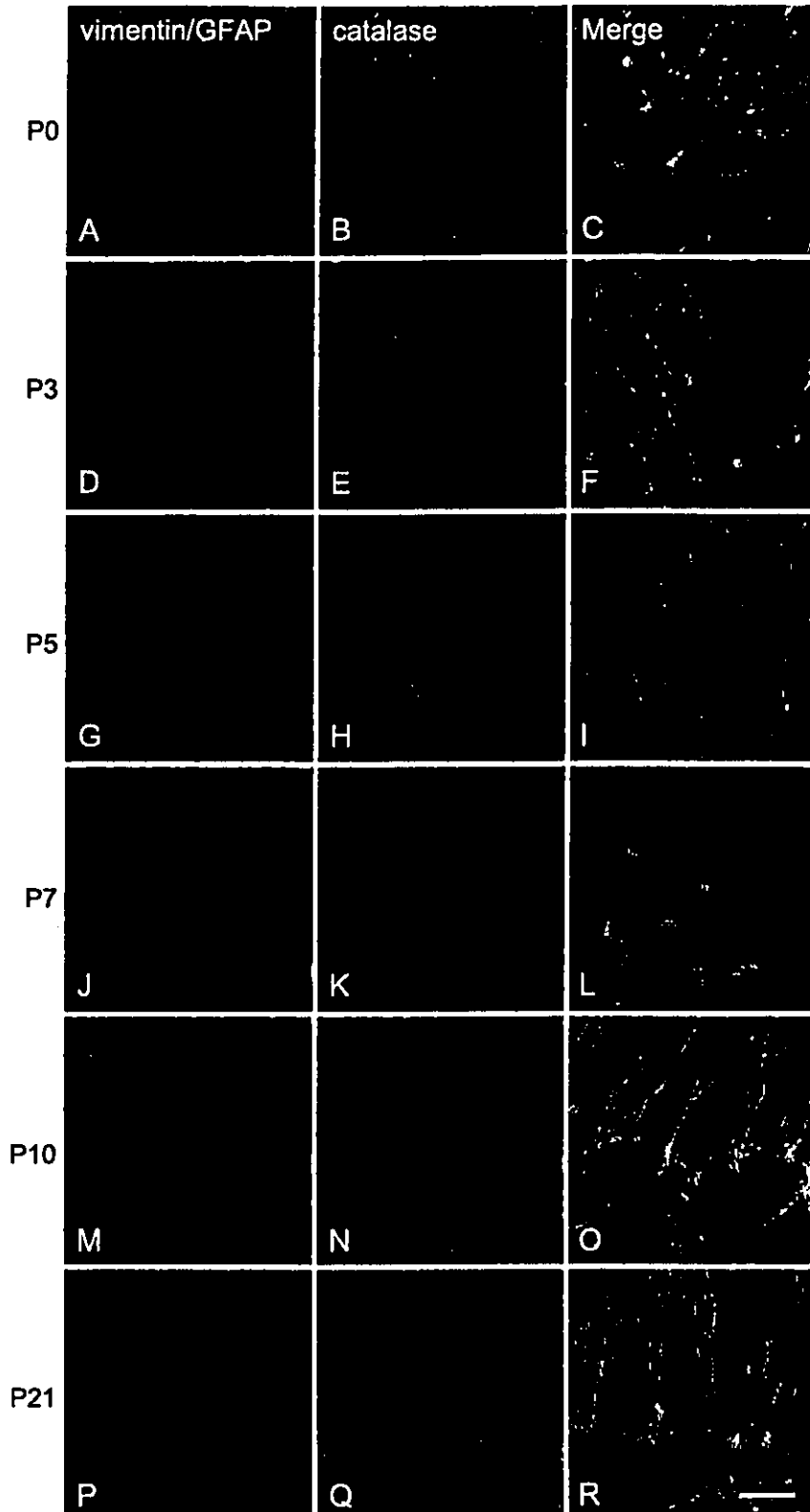
Fig. 2. Double immunofluorescence for vimentin (A, D and G)/GFAP (J, M and P) and catalase (B, E, H, K, N and Q) in the cerebellar cortex on the each postnatal day. All images were taken near the midpoint of the preculminate fissure. On P10 and P21, GFAP is evident because as on these days vimentin in the molecular layer was little evident. The punctate patterns of catalase (peroxisomes) are co-localized with vimentin/GFAP, especially in soma of Bergmann glia. On P10 and 21, peroxisomes are co-localized with the radial pattern of Bergmann glia (O and R). Scale bar indicates 20 μm.

To clarify the localization of catalase-positive peroxisomes in Purkinje and glial cells, double immunostaining for catalase, IP3R and vimentin/GFAP was done. On double immunostaining for catalase and IP3R, peroxisomes were rarely evident in Purkinje cells (Fig. 1C, F, I, L, O and R). On double immunostaining for catalase and glial markers, numerous peroxisomes were distributed mainly in somata and fibers of the Bergmann glia (Fig. 2C, F, I, L, O and R).
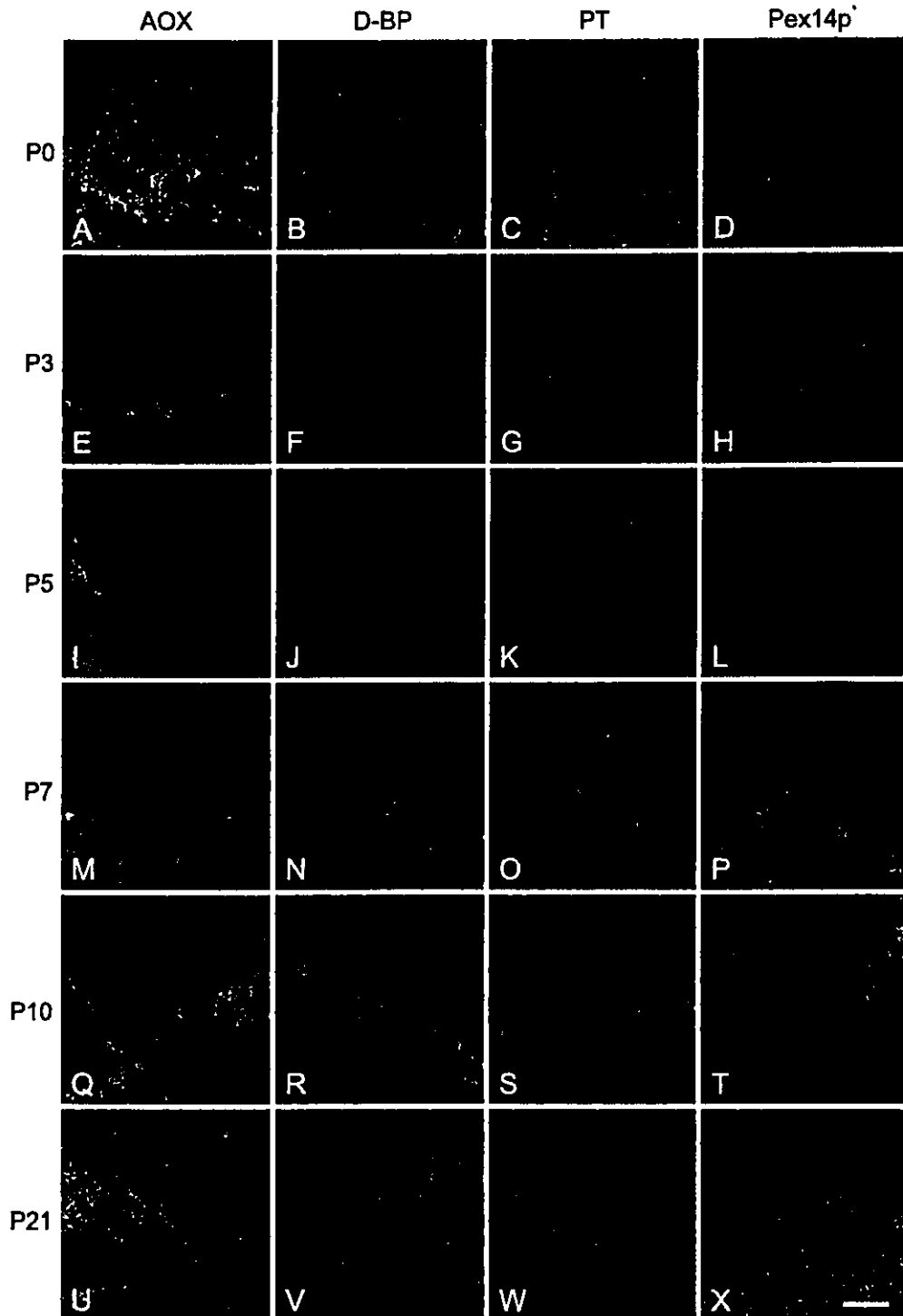

Fig. 3. Immunofluorescence for acyl-CoA oxidase (AOX) (A, E, I, M, Q and U), D-bifunctional protein (D-BP) (B, F, J, N, R and V), 3-ketoacyl-CoA thiolase (PT) (C, G, K, O, S and W) and Pex14p (D, H, L, P, T and X) in the cerebellar cortex on the each postnatal day. All images were taken near the midpoint of the preculminate fissure. Few peroxisomes are seen in Purkinje cells in immunostaining for AOX, D-BP and PT, like immunostaining for catalase. Numerous peroxisomes are seen in immunostaining for Pex14p. Scale bar indicates 20 μm.

Double immunostaining for catalase and vimentin was evident in P0, P3 and P5, and for catalase and GFAP, in P7, P10 and P21.

To clarify if empty peroxisomal structures were evident in Purkinje cells, we did immunostaining for Pex14p, one of the peroxisomal membrane proteins. Many particles were evident in somata of Purkinje cells of all ages of cells (Fig. 3D, H, L, P, T and X).

3.2. Cell cultures

On double immunostaining with anti-catalase and calbindin antibodies, few peroxisomes were detected in calbindin-positive cells, Purkinje cells (Fig. 4A–C). In case of

Table 1
Proportion of cells with catalase-positive particles

	Total	–	+	++	+++
Calbindin-positive cells (%)	25 (100.0)	8 (32.0)	15 (60.0)	2 (8.0)	0 (0.0)
GFAP-positive cells (%)	98 (100.0)	0 (0.0)	0 (0.0)	0 (0.0)	98 (100.0)

(–) none; (+) weakly positive; (++) positive; (+++) strongly positive.

immunostaining with anti-catalase and GFAP antibodies, numerous peroxisomes were seen in GFAP-positive cells, glial cells (Fig. 4D–F). We counted calbindin- and GFAP-positive cells in the each area and examined the catalase-positive particles (Table 1). All of the GFAP-positive cells
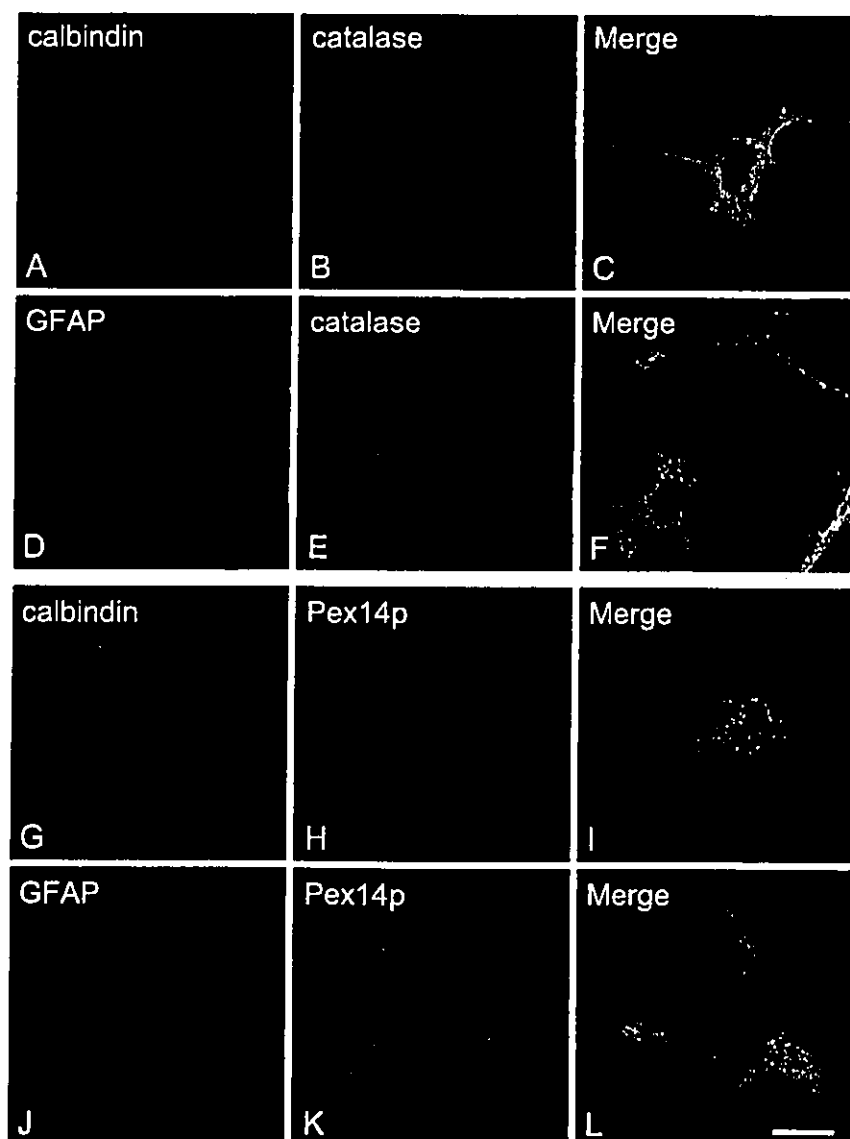

Fig. 4. (A, B, C) Double immunofluorescence for calbindin (red) and catalase (green). (D, E, F) Double immunofluorescence for GFAP (red) and catalase (green). (G, H, I) Double immunofluorescence for calbindin (red) and Pex14p (green). (J, K, L) Double immunofluorescence for GFAP (red) and Pex14p (green). In immunostaining for catalase, few peroxisomes are detected in calbindin-positive cells (Purkinje cells) (A–C), however, numerous peroxisomes are seen in GFAP-positive cells (glial cells) (D–F). In immunostaining for Pex14p, numerous peroxisomes are also seen in Purkinje cells (G–I), as glial cells (J–L). Scale bar indicates 20 μm.

had strongly catalase-positive particles, whereas catalase-positive particles in the calbindin-positive cells were fewer in number.

On immunostaining for Pex14p, peroxisomes were evident in somata of Purkinje cells as in glial cells (Fig. 4G–L). The number and apparent size of peroxisomes as seen with immunostaining with Pex14p antibodies, seemed to be equal in Purkinje (Fig. 4G–I) and glial cells (Fig. 4J–L).

4. Discussion

Immunohistochemical studies on peroxisomal proteins, either in the adult or in developing mammal nervous tissues (human, rat or mouse, respectively), have been done by immunostaining not only for catalase [10–12], but also for other proteins. There is very wide diversity regarding the population and intracellular localization of peroxisomes, in targeted proteins and with aging. Proteins containing peroxisomes differ from the case of an intracellular localization and its own size [13,14].

In the present work, we found that peroxisomes contained catalase in Bergmann glia, yet none or fewer in Purkinje cells, in case of both frozen sections and cultured cells from the developing mouse cerebellum. We did the same experiments on adult mice (about postnatal days 100). In Purkinje cells, punctate patterns of catalase were also few, as on P21 (data not shown). Furthermore, few immunostained particles were seen in Purkinje cells using antibodies for additional peroxisomal matrix proteins containing both PTS1 and PTS2 motif, however, the peroxisomal membrane structure was found in Purkinje cells using immunostaining for Pex14p as well as in Bergmann glia. Peroxisomes in Purkinje cells may have little function because matrix proteins can fail to be imported into peroxisomes in Purkinje cells. In previous studies on fibroblasts in cases of Zellweger syndrome, the empty membrane structures were of larger size [15], and those fibroblasts were affected by protein import into the peroxisomes by the mutated PEX genes [1]. We considered that the mechanisms of impaired peroxisome protein import in Purkinje cells may be not the same as the Zellweger fibroblasts, however, the different expression of PEX genes between Purkinje cells and Bergmann glia may be clue to clarify the peroxisomal metabolism in the central nervous system (CNS).

Some interactions between Purkinje cells and Bergmann glia have been noted in the developing cerebellum [8,16–19]. In the vimentin null mouse with poorly developed and highly abnormal Bergmann glia, the Purkinje cell had a paucity of spiny branchlets and disorganized dendrites and were hypertrophic with a massive thickening of processes. This means stunting of Purkinje cells may be caused by dysfunction of the Bergmann glia [8]. Regarding a structural relationship between radial fibers and migrating Purkinje cells, radial-glial fibers are apposed to and are in contact with calbindin-positive Purkinje cells at embryonic days 14

and 15. Radial glial processes are involved, not only in the contact guidance of Purkinje cell migration through expression of cell adhesion molecules, but also in the tropic support of the apposed immature neurons by means of cell adhesion and molecular transfer through the sequestration of various molecules into the vesicles [16]. Postnatally, Bergmann fibers surround synapses of Purkinje cells almost completely [17,18]. In the mammalian CNS, astroglia may play a pivotal role in the metabolism of L-serine, and 3-phosphoglycerate dehydrogenase (3PGDH), an enzyme essential for L-serine biogenesis, is highly expressed in Bergmann glia but apparently not expressed in Purkinje cells [19].

Some murine models with targeted disruption of PEX genes have been described [20–24]. The deficient PEX2 mouse, with a genetic background; Swiss Webster (SW) × 129 Svev (Sw/129), has a significant postnatal survival, with approx. 20–30% of mice surviving for 7–10 days and a lower rate of survival of P12–13 [22]. While the control of cerebellar foliation pattern is poorly understood, the dendritic growth of underlying Purkinje cells is considered to be an important contributing factor. Size of the Purkinje cell dendritic arbor and the degree of branching were markedly reduced in the P9 of PEX2-deficient mice. PEX2 mutant mice had severe abnormalities in the Purkinje cell dendritic arborization throughout the cerebellum. There was often a single large dendrite that did not branch throughout much of its course in the molecular layer. Portions of the dendritic trees were often present near the mutant Purkinje cell soma, which had an irregular contour. Many of the thick proximal dendrites in the mutants were studded with spines. There was also an increased spine density on distal dendrites in the mutants. Thus, peroxisome deficiency plays a prominent role in dendritic growth and maturation of the large Purkinje cells in the cerebellum.

All this evidence suggests that Purkinje cells may depend on peroxisomal metabolism mainly in Bergmann glia, and peroxisomes in glial cells may have an important role in the development of neuron–glial interactions bringing about the maturation of Purkinje cells. We intend to investigate peroxisomal metabolism and PEX gene expression in isolated Purkinje cells.

Acknowledgements

References

[1] S.J. Gould, G.V. Raymond, D. Valle, The peroxisomal biogenesis disorders, in: C.R. Scriver, A.L. Beaudet, W.S. Sly, D. Valle (Eds.), The Metabolic and Molecular Bases of Inherited Disease, eight edition, McGraw-Hill, New York, 2001, pp. 3181–3217.

[2] S. Naidu, C. Theda, H.W. Moser, Peroxisomal disorders, in: K.F. Swaiman, S. Ashwal (Eds.), Pediatric Neurology: Principles and Practice, third edition, Mosby, St. Louis, 1999, pp. 510–529.

[3] J.M. Powers, H.W. Moser, Peroxisomal disorders: genotype, phenotype, major neuropathologic lesions, and pathogenesis, Brain Pathol. 8 (1998) 101–120.

[4] N. Shimozawa, T. Tsukamoto, Y. Suzuki, T. Orii, Y. Shirayoshi, T. Mori, Y. Fujiki, A human gene responsible for Zellweger syndrome that affects peroxisome assembly, Science 255 (1992) 1132–1134.

[5] N. Shimozawa, Z. Zhang, Y. Suzuki, A. Imamura, T. Tsukamoto, T. Osumi, Y. Fujiki, T. Orii, P.G. Barth, R.J. Wanders, N. Kondo, Functional heterogeneity of C-terminal peroxisome targeting signal 1 in PEX5-defective patients, Biochem. Biophys. Res. Commun. 262 (1999) 504–508.

[6] Y. Huang, R. Ito, T. Imanaka, N. Usuda, M. Ito, Different accumulations of 3-ketoacyl-CoA thiolase precursor in peroxisomes of Chinese hamster ovary cells harboring a dysfunction in the PEX2 protein, Biochim. Biophys. Acta 1589 (2002) 273–284.

[7] M. Yuzaki, K. Mikoshiba, Y. Kagawa, Cerebellar astrocytes specifically support the survival of Purkinje cells in culture, Biochem. Biophys. Res. Commun. 197 (1993) 123–129.

[8] E. Colucci-Guyon, Y.R.M. Gimenez, T. Maurice, C. Babinet, A. Privat, Cerebellar defect and impaired motor coordination in mice lacking vimentin, Glia 25 (1999) 33–43.

[9] S. Nakagawa, M. Watanabe, T. Isobe, H. Kondo, Y. Inoue, Cytological compartmentalization in the staggerer cerebellum, as revealed by calbindin immunohistochemistry for Purkinje cells, J. Comp. Neurol. 395 (1998) 112–120.

[10] G. Arnold, E. Holtzman, Microperoxisomes in the central nervous system of the postnatal rat, Brain Res. 155 (1978) 1–17.

[11] S. Houdou, S. Takashima, Y. Suzuki, Immunohistochemical expression of peroxisomal enzymes in developing human brain, Mol. Chem. Neuropathol. 19 (1993) 235–248.

[12] S. Moreno, E. Mugnaini, M.P. Ceru, Immunocytochemical localization of catalase in the central nervous system of the rat, J. Histochem. Cytochem. 43 (1995) 1253–1267.

[13] F. Fouquet, J.M. Zhou, E. Ralston, K. Murray, F. Troalen, E. Magal,
O. Robain, M. Dubois-Dalcq, P. Aubourg, Expression of the adrenoleukodystrophy protein in the human and mouse central nervous system, Neurobiol. Dis. 3 (1997) 271–285.

[14] A.M. Cimini, I. Singh, S. Farioli-Vecchioli, L. Cristiano, M.P. Ceru, Presence of heterogeneous peroxisomal populations in the rat nervous tissue, Biochim. Biophys. Acta 1425 (1998) 13–26.

[15] M.J. Santos, T. Imanaka, H. Shio, G.M. Small, P.B. Lazarow, Peroxisomal membrane ghosts in Zellweger syndrome-aberrant organelle assembly, Science 239 (1988) 1536–1538.

[16] S. Yuasa, K. Kawamura, R. Kuwano, K. Ono, Neuron–glia interrelations during migration of Purkinje cells in the mouse embryonic cerebellum, Int. J. Dev. Neurosci. 14 (1996) 429–438.

[17] K. Yamada, M. Fukaya, T. Shibata, H. Kurihara, K. Tanaka, Y. Inoue, M. Watanabe, Dynamic transformation of Bergmann glial fibers proceeds in correlation with dendritic outgrowth and synapse formation of cerebellar Purkinje cells, J. Comp. Neurol. 418 (2000) 106–120.

[18] K. Yamada, M. Watanabe, Cytodifferentiation of Bergmann glia and its relationship with Purkinje cells, Anat. Sci. Inst. 77 (2002) 94–108.

[19] S. Furuya, T. Tabata, J. Mitoma, K. Yamada, M. Yamasaki, A. Makino, T. Yamamoto, M. Watanabe, M. Kano, Y. Hirabayashi, L-Serine and glycine serve as major astroglia-derived trophic factors for cerebellar Purkinje neurons, Proc. Natl. Acad. Sci. 97 (2000) 11528–11533.

[20] M. Baes, P. Gressens, E. Baumgart, P. Carmeliet, M. Casteels, M. Fransen, P. Evrard, D. Fahimi, P.E. Declercq, D. Collen, P.P. van Veldhoven, G.P. Mannaerts, A mouse model for Zellweger syndrome, Nat. Genet. 17 (1997) 49–57.

[21] P.L. Faust, M.E. Hatten, Targeted deletion of the PEX2 peroxisome assembly gene in mice provides a model for Zellweger syndrome, a human neuronal migration disorder, J. Cell Biol. 139 (1997) 1293–1305.

[22] P.L. Faust, H.M. Su, A. Moser, H.W. Moser, The peroxisome deficient PEX2 Zellweger mouse: pathologic and biochemical correlates of lipid dysfunction, J. Mol. Neurosci. 16 (2001) 289–297.

[23] X. Li, E. Baumgart, J.C. Morrell, G. Jimenez-Sanchez, D. Valle, S.J. Gould, PEX11 beta deficiency is lethal and impairs neuronal migration but does not abrogate peroxisome function, Mol. Cell. Biol. 22 (2002) 4358–4365.

[24] X. Li, E. Baumgart, G.X. Dong, J.C. Morrell, G. Jimenez-Sanchez, D. Valle, K.D. Smith, S.J. Gould, PEX11alpha is required for peroxisome proliferation in response to 4-phenylbutyrate but is dispensable for peroxisome proliferator-activated receptor alpha-mediated peroxisome proliferation, Mol. Cell. Biol. 22 (2002) 8226–8240.